6

Soil Colloidal Behavior

Sabine Goldberg, Inmaculata Lebron, and D.L. Suarez
USDA-ARS, U.S. Salinity Laboratory

6.1 Nature of Soil Colloids

6.1.1 Significance of Colloidal Phenomena

The importance of colloids in soil science has been appreciated for many years. However, recent understanding that organic and inorganic contaminants are often transported via colloidal particles has increased interest in colloid science. Essentially, all chemicals and individual species are to some extent reactive with soils, including species such as Cl^-, which undergo repulsion from negatively charged surfaces. With few exceptions, soil chemistry is primarily the chemistry of colloids and surfaces. The primary importance of colloids in soil science stems from their surface reactivity and charge characteristics. The overwhelming majority of surface area and electrostatic charge in a soil resides in the less than 1 μm size fraction, with particles with radii between 20 and 1,000 nm constituting the major part of the soil surface area (Borkovec et al., 1993).

Characterizations of size, shape, surface area, surface charge density and changes in surface charge are required for understanding the processes of adsorption, flocculation, dispersion, and transport in soils and the resultant changes in soil hydraulic properties as well as chemical migration. Since the major part of the surface area is in the colloidal fraction of the soil, almost all surface-controlled processes including adsorption reactions, nucleation and precipitation/dissolution involve colloids. Colloids are reactive not only because of their total surface area but because of enhanced reactivity related to rough surfaces and highly energetic sites, as well as the effects of electrostatic charge. Colloid charge is associated with substitution of lower charge cations for those of higher charge in the mineral lattice (which results in a net permanent charge) as well as surface charge associated with broken bonds. The charge associated with broken bonds is characterized as variable charge in as much as the solution influences the surface speciation (Section B, Chapter 7). In addition to these chemical processes, colloids are mobile in soils, and thus affect not only the chemical transport of otherwise immobile chemicals, but also exert a strong influence on soil hydraulic properties.

6.1.2 Types of Soil Colloids

Colloidal particles are defined as having an equivalent spherical radius smaller than 1 μm (van Olphen, 1977). A homogeneous dispersion of colloidal particles in a liquid is called a colloidal dispersion. If the particles are large and settle rapidly, the dispersion is called a suspension. A colloidal dispersion

is defined as a system where particles of colloidal dimensions are dispersed in a continuous phase of a different composition (van Olphen, 1977).

6.1.2.1 Oxides

Oxides including hydroxides and oxyhydroxides are ubiquitous constituents of soils occurring as both discrete particles and as coatings on other soil surfaces. Oxide minerals that are commonly found in the soil clay fraction are discussed in Section F, Chapter 3.

Hydroxylation of oxide minerals can either be structural and/or by chemisorption of water in an aqueous medium (Schwertmann and Taylor, 1977). Edge hydroxyl groups on oxide and clay minerals represent the most abundant and reactive surface functional groups in soils (Sposito, 1984). Any one type of oxide mineral contains various groups of surface hydroxyls that are distinguishable by crystal plane location and/or extent of coordination to the cations of the bulk structure. However, as a simplification it is often assumed that each oxide mineral has a single set of homogeneous functional groups. Surface hydroxyl groups on most oxide minerals are amphoteric, exhibiting positive charge at low pH and negative charge at high pH. For this reason oxide minerals are often referred to as variable charge soil minerals. Table 6.1 provides densities of surface hydroxyl groups for some common oxide minerals in soils.

Boehmite and gibbsite are the only crystalline Al oxides common in soils. Aluminum oxides are the products of intense weathering of aluminosilicate minerals and are most abundant in tropical soils. Gibbsite can also be found in volcanic ash soils of humid regions (Brown et al., 1978). Noncrystalline Al oxides, which have similar structure and chemical characteristics but smaller particle size than crystalline varieties, often dominate the chemical reactions with anions in soils (Hsu, 1977). Aluminum oxides play an important role in ion adsorption, stabilization of aggregates, and flocculation of soil particles.

Iron oxides are found in most soils, providing soil horizons with their red, yellow, and brown colors (Brown et al., 1978). Goethite, which is the most common Fe oxide in temperate, subtropical, and tropical soils, is usually thermodynamically the most stable (Schwertmann and Taylor, 1977). Soil goethites are usually fine grained and contain appreciable substituted Al. Lepidocrocite is a minor constituent of waterlogged temperate soils undergoing alternating oxidizing and reducing conditions while hematite is a common soil mineral that can be inherited from parent materials or formed pedogenically in warm regions (Brown et al., 1978). Two magnetic Fe minerals, magnetite and maghemite, occur in soils; the former being inherited from parent rock, while the latter is formed

Table 6.1 Densities of surface hydroxyl groups on oxide minerals [Adapted from Davis and Kent, 1990]

Solid	Site density range (sites nm^{-2})
Gibbsite	2-12
Goethite	2.6-16.8
Hematite	5-22
Ferrihydrite	1.1-10.1
MnO_2	6.2
TiO_2	2-12
Amorphous SiO_2	4.5-12

pedogenically in highly weathered soils (Brown et al., 1978). Ferrihydrites are poorly crystalline, have indefinite composition, and occur as very small particles with high surface area (Schwertmann and Taylor, 1977). Ilmenite is an uncommon mineral usually inherited from igneous or metamorphic parent rocks (Brown et al., 1978). Iron oxides play an important role in ion adsorption and aggregation and cementation of soil particles.

Manganese oxides which supply Mn for plants occur widely in soils as minor constituents, mainly as dark coatings on particle surfaces. Manganese oxides are chemically complex, existing as a continuous range of compositions between MnO and MnO_2 (Brown et al., 1978). Birnessite, vernadite, lithiophorite, and hollandite are the most common crystalline manganese minerals in soils (McKenzie, 1989). Birnessite occurs in both acid and alkaline soils, while lithiophorite occurs mainly in neutral to acid soils (Brown et al., 1978). Manganese oxides exhibit a strong adsorption capacity for metal cations, especially Cu, due to their variable charge, small particle size, and large surface area (McKenzie, 1989).

Rutile and anatase, the common Ti oxides in soils, are the high and low temperature forms, respectively, the former occurring in igneous and metamorphic rocks and the latter as an alteration product of Ti-containing minerals such as ilmenite, much less abundant than rutile (Hutton, 1977; Brown et al., 1978). Titanium oxides are present in both the coarse and fine fractions of soils and are very insoluble (Hutton, 1977).

Quartz is not only the most abundant Si oxide but also the most abundant mineral in most soils. Most quartz is found predominantly in the sand, silt, and coarse clay fraction of soils (Wilding et al., 1977). Silicon oxides are generally considered inert having a small surface area and little surface charge.

6.1.2.2 Clay Minerals

The clay fraction of most soils is dominated by various layer silicate clay minerals. Layer silicate clay minerals are classified as 1:1 where each layer consists of one tetrahedral silica sheet and one octahedral alumina sheet, 2:1 where each layer consists of one octahedral sheet sandwiched between two tetrahedral sheets, or 2:1:1 where a metal hydroxide sheet is sandwiched between the 2:1 layers. Layer silicate minerals common in soils are discussed in Section F, Chapter 2. A discussion of silicate structures is provided by Schulze (1989).

Layer silicate clay minerals are characterized by isomorphic substitution of lower valence cations in either or both the tetrahedral and octahedral sheets. This excess of negative charge is balanced by other cations, either inside the crystal or on the external surface (McBride, 1994). Layer charge is charge that is balanced outside of the structural unit and determines the strength and type of bonding occurring between the basal planes. Charge arising from isomorphic substitution is called permanent charge because it is independent of solution pH. Layer silicate clay minerals also possess variable charge located at the broken edges of clay particles. At the edges of the octahedral sheet, hydroxyl ions attached to Al cations are called aluminol groups. Similar to the hydroxyl groups on oxide minerals, aluminol groups are amphoteric. At the edges of the tetrahedral sheet hydroxyl groups attached to Si cations are called silanol groups. Silanol groups do not undergo protonation, but dissociate and become negatively charged at high pH. Adsorbed cations on clay minerals balance both variable and permanent charge. Table 6.2 provides charge characteristics and cation exchange capacities (CEC) for some common clay minerals in soils.

Kaolinite is one of the most widespread clay minerals in soils, being most abundant in soils of warm moist climates (Dixon, 1977); while halloysite is formed through acid weathering and in soils of volcanic origin. The halloysite structure is the same as the kaolinite structure but contains a sheet of water molecules between the layers. Both have low colloidal activity, surface area, and CEC and anion

Table 6.2 Charge characteristics and cation exchange capacities of clay minerals [Bohn et al., 1985; McBride, 1994]

Solid	Charge per unit half cell		Cation exchange capacity ($cmol_c\ kg^{-1}$)
	Tetrahedral	Octahedral	
Kaolinite	0	0	1-10
Smectite			80 -120
Montmorillonite	0	–0.33	
Beidellite	–0.5	0	
Vermiculite	–0.85	+0.23	120 -150
Mica			20 - 40
Muscovite	–0.89	–0.05	
Chlorite			10 - 40

exchange capacities (AEC) (Dixon, 1977) which are predominantly variable in nature (McBride, 1994).

Micas are abundant in soils, occurring as primary minerals inherited from soil parent materials. Micas strongly retain interlayer K ions, rendering them nonexchangeable and reducing the CEC of these minerals. Through weathering, micas release K and provide an important natural source of this plant nutrient (Fanning and Keramidas, 1977). Illite is a secondary mineral that is less crystalline, contains less K, and more water than muscovite mica (McBride, 1994). Micas and illites are nonswelling minerals.

Smectites constitute an important group of 2:1 clay minerals. Members that are important in soils include montmorillonite, beidellite, and nontronite. Smectites are most significant in moderately weathered soils and have high colloidal activity and surface area. Smectites are responsible for a large part of the CEC and the majority of the shrink/swell properties of smectitic soils (Borchardt, 1977).

Vermiculite is an important clay mineral in soil that is formed as an alteration product of muscovite and biotite micas (Douglas, 1977). Vermiculite, which is widely distributed and has a wide particle size range, contains hydrated Mg cations that can be readily exchanged by K and NH_4 ions, resulting in collapse of the clay layers and fixation of these nutrient ions. Vermiculites have high CEC and surface area but exhibit limited swelling.

Chlorites are 2:1:1 layer silicates that occur extensively in soils. The hydroxide interlayer sheet is usually dominated either by brucite [$Mg(OH)_2$] or by gibbsite [$Al(OH)_3$]. This interlayer sheet restricts swelling, decreases effective surface area and effective cation exchange capacity (ECEC) (McBride, 1994). Chlorites are nonswelling silicates.

6.1.2.3 Organic Matter

Soil organic matter (SOM) refers to the mixture of products resulting from microbial and chemical transformations of organic residues and is discussed in Section B, Chapter 2. Humus is a complex and microbially resistant mixture of amorphous and colloidal substances modified from original tissues or synthesized by soil microorganisms. Humic substances are subdivided into humic acid, fulvic acid,

and humin using a separation scheme based on solubility in strong acid and base (McBride, 1994). The structure and composition of humus are complex and incompletely known. The structure contains a variety of reactive functional groups including carboxyl R–COOH, phenol C_6H_5OH, alcohol R–CH_2OH, enol R–CH=CH–OH, ketone R–CO–R′, quinone $O=C_6H_4=O$, ether R–CH_2–O–CH_2–R′, and amino R–NH_2 (Stevenson, 1982). Humus is amorphous and highly colloidal; its surface area, ion adsorption and CEC are greater than those of layer silicate clay minerals (McBride, 1994). The presence of humus usually promotes aggregation of soil particles.

6.1.3 Properties of Soil Colloids

6.1.3.1 Particle Size and Shape

Colloids in natural systems are characterized by a continuous particle size distribution of extreme complexity and diversity. Organisms, organic macromolecules, clays, oxides and combinations of any of them constitute the colloidal fraction in soils. The distribution of shapes, densities, surface chemical properties, and chemical composition may vary widely with size. Some fractions of the size spectrum may be living, and all particulates are subject to diverse physical, chemical and biological processes that can alter size distribution, shape, or chemical composition (Kavanaugh and Leckie, 1980).

Colloids are dynamic particles; the distribution of particle sizes in natural systems is the result of a number of processes, which either bring the particles together (coagulation mechanisms) or disrupt existing aggregates (Filella and Buffle, 1993; Buffle and Leppard, 1995a,b). Sequential gravimetric analysis following filtration or centrifugation is the classical method for measuring particle size distributions in colloidal systems. However, this technique does not provide a reliable size distribution for particles less than 1 μm. Techniques such as electron microscopy and light scattering methods are better suited for submicron particle sizing. High resolution transmission electron microscopy (HRTEM) and photon correlation spectroscopy (PCS) are promising techniques for this size range, provided that artifacts are minimized (Filella and Buffle, 1993).

Minimization of sample handling and processing is recommended when analyzing colloidal systems. Unfortunately, no *in situ* technique that allows direct measurement of the particle size distribution has yet been developed. Furthermore, most of the methods commercially available do not allow quantification of small particles in the presence of a high proportion of larger particles, a condition frequently found in soils. A combination of fractionation techniques and other methods of analysis is advised due to the unstable nature of the system under study (Filella and Buffle, 1993).

Measurement of colloid particle size distribution is challenging because of the heterogeneous characteristics of particulates. Shape, density, refractive index, and other physical properties are usually nonuniform throughout the six to seven orders of magnitude size range of the particulate fraction. No single measurement technique is able to measure the particle size distribution over this wide size range (Kavanaugh et al., 1980). The interpretation of these measurements is further complicated because changes in the size distribution occur due to particle aggregation or breakup during sampling or sample preparation.

Measurement Methodology

There are many methods to determine the particle size distribution of a soil sample. These methods can be divided into direct and indirect methods. Direct methods are those that provide information by direct observations. In this category, all the microscopic and ultramicroscopic techniques are included. Indirect methods, which are more extensively used, determine the size of the particles in dispersions. Certain bulk physical properties of the suspensions are measured and the average particle dimensions are computed on the basis of theoretical relations between particle dimensions and

physical properties. The following physical properties of suspensions have been used for the evaluation of particle size and shape: sedimentation velocity, viscosity, decay of optical birefringence induced by an orientation of the particles in an electric field, dynamic light scattering, intensity of transmitted light, and low angle X-ray scattering, among others (van Olphen, 1977; Hunter, 1993). All of these techniques have intrinsic assumptions and limitations. It is not unusual to obtain different particle size distributions for the same sample using different techniques.

Electron Microscopy

The electron microscope is the only instrument capable of measuring the size of particles in the colloidal range (1 nm to 1 μm). Both the transmission and scanning electron microscopes require sample evacuation and in most cases coating of the particulates with a conducting material, typically carbon or gold. Thus sample preparation can alter the original particle size distribution, unless freeze drying techniques are used. From the weight concentration of the suspension and the number of particles in a given volume, the average weight of a single particle can be calculated (van Olphen, 1977). New techniques, such as image analysis, facilitate the quantification of particle sizes with electron microscopy. These methods are not widely used for routine particle size analysis because of the high cost of this equipment. Additionally, detection limits are poor, because small sample volumes are scanned at any given magnification. Despite this limitation, microscopy remains the essential technique for determination of particulate shape factors.

Sedimentation. The steady-state velocity of a particle in suspension, settling in the gravitational field, is given by:

$$M_e g = f\left(\frac{dx}{dt}\right) \qquad [6.1]$$

where M_e is the effective particle mass, f is the frictional coefficient, dx/dt is the particle velocity, and g is the gravitational acceleration. Steady-state velocities are normally expressed in terms of the sedimentation coefficient (S). Thus, for Equation [6.1],

$$S = \frac{1}{g}\frac{dx}{dt} = \frac{M_e}{f} \qquad [6.2]$$

The sedimentation coefficient is the ratio between the particle effective mass and the frictional coefficient. The relationship between sedimentation data and particle size is a function of the particle shape and density and the density and viscosity of the medium. The results from a sedimentation experiment can be given as a distribution of S. If the particle density (ρ) and the density of the medium (ρ_0) are known, S can be expressed as:

$$S = \frac{V(\rho - \rho_0)}{f} \qquad [6.3]$$

where V is the particle volume. Assuming that the particles are spherical with the frictional coefficient given by Stokes' Law as $f = 3\pi_0\eta d_p$, the sedimentation coefficient for a particle of diameter d_p suspended in a medium with viscosity (η), then becomes:

$$S = \frac{V(\rho_- \rho_0)d_p^2}{18\eta} \qquad [6.4]$$

from which the particle diameter may be calculated.

For particles other than spheres, similar expressions can be obtained using frictional coefficients appropriate to the particle dimensions and geometry. A more detailed theoretical treatment is provided in Jackson (1979) and Bunville (1984).

A particle falling through an infinite fluid will eventually fall at a terminal constant velocity determined by the size of the particle and the resistance offered by the fluid. In a centrifugal field, the terminal velocity is not constant, because the centrifugal field is a function of the centrifugal radius. Measurement of the terminal velocity is necessary in order to calculate the particle size. The relationship between the movement of the particle and the movement of fluid around that particle may be reduced to the Stokes equation. For fluid moving past a particle of diameter (d_p), the ratio of the inertial transfer is described by the dimensionless parameter, the Reynolds number (R_E):

$$R_E = \frac{\rho_0 u d_p}{\eta} \qquad [6.5]$$

where u is the velocity. If $R_E \leq 0.2$, the fluid conditions are described as streamlined or laminar, and the drag on the particle is due mainly to viscous force within the fluid. Particles with high densities or large particle diameters may be moving with velocities that exceed $R_E = 0.2$, and in this situation, are likely to enter the region of turbulent flow, where velocities are more difficult to calculate.

In a centrifugal field, Stokes' equation has the form:

$$u = \frac{(\rho - \rho_0)\omega^2 d_p^2}{18\eta} = \frac{\ln(r / S_0)}{t} \qquad [6.6]$$

where ω is the rotational velocity (rad s^{-1}) and t is the time (s) required for a particle of diameter d_p to move from its starting point radius (S_0) to the analytical radius (r).

Application of the Stokes equation requires certain assumptions that are not always achieved. All these assumptions are critical to the measurement of the size of the sedimenting particles. The first assumption is that the particles are spherical, smooth, and rigid. Since this is almost never valid, the diameter calculated is an equivalent or Stokes diameter (d_{St}). It is assumed that the particle terminal velocity is reached instantly, although calculations show that a finite but small time period is actually required before this condition is reached. The particle is assumed to be moving without interference or interaction from other particles in the system. This assumption is only true at high dilutions (< 1%) that ensure considerable separation between the particles. Also, it is assumed that inertial effects are not present and that the fluid only exhibits Newtonian flow properties. Since water is generally the dilution medium in soils and colloidal particles are < 1 μm, these assumptions are usually valid.

A more detailed analysis of the methodology as well as a description of different centrifugation methods are provided in Bunville (1984), Groves (1984), Koehler et al. (1987), Holsworth et al. (1987), and Coll and Oppenheimer (1987).

Electrical Properties

The increase in the resistance across a small aperture produced by a nonconducting particle in a conducting medium is called the Coulter effect. The magnitude of this increase in resistance (ΔR) for a spherical particle of diameter (d_p) suspended in an aperture of diameter (D_a) is

$$\Delta R = \frac{8P_f d_p}{3\pi D_a^4}\left[1 + \frac{4}{5}\left(\frac{d_p}{D_a}\right)^2 + \frac{24}{35}\left(\frac{d_p}{D_a}\right) + \ldots\right] \qquad [6.7]$$

where P_f is the resistivity of the conducting medium. This resistance pulse (ΔR) results in a voltage pulse ($i\Delta R$) for a sphere of diameter d_p, where i is the current across the aperture. The resulting voltage pulses are counted and scaled using a multichannel analyzer.

Instruments utilizing the resistive pulse technique require calibration using standards of particles with known diameter to assign a particle size to each of the thresholds. This procedure takes into account the dimensions and electrical characteristics of the aperture and the conducting medium.

The advantage of the resistive pulse technique is that no other property of the particle, such as refractive index or specific gravity, is required for the interpretation of the data in terms of a particle size distribution. Developments in instrumentation for particle size analysis using the resistive pulse technique allow the analysis of particle sizes < 1 μm (Bunville, 1984).

Photon Correlation Spectroscopy

Photon correlation spectroscopy (PCS) or dynamic light scattering measures the fluctuation in scattered intensity of a laser beam over small time intervals when it passes through a small volume of particles under Brownian motion. The polarized intensity (I_{vv}) time correlation function is given by the expression (Pecora, 1983; Schurtenberger and Newman, 1993):

$$\langle I_{vv}(0) I_{vv}(t) \rangle = A = B\exp\left[-2q^2 D_t \tau\right] \qquad [6.8]$$

where A and B are constants, τ is the delay time, D_t is the translational diffusion coefficient, and q is the length of the scattering vector, which is related to the wavelength of the incident light (λ) and the scattering angle (θ) by the expression:

$$q = 4\frac{\pi}{\lambda}\sin\left(\frac{\theta}{2}\right) \qquad [6.9]$$

Assuming that the particles are spheres, this translational diffusion constant is related to the radius (r) of the particle according to the Stokes-Einstein relationship at infinite dilution:

$$D_t = k_B \frac{T}{6\pi\eta r} \qquad [6.10]$$

where k_B is the Boltzmann constant and T is the absolute temperature (Pecora, 1983).

When the particles have a regular shape other than spherical, the depolarized component is used to study the particle rotational diffusion coefficient. The rotational and translational diffusion

coefficients obtained in conjunction with theoretical, hydrodynamic relationships contain information on the particle dimensions.

For a nonspherical particle larger than the incident wavelength, light is scattered from different parts of the same particle producing interferences which are dependent on the angle of the scattered intensity and characteristic of a particular particle shape. The time dependence of fluctuations in orientation, shape, or size is important and cannot be observed unless the fluctuation exhibits a sufficiently large amplitude, compared to q^{-1}, for the different states (Pecora, 1983).

When the particles are not spheres or have no unique shape the theoretical model is complex. Despite limitations, PCS has been applied to measure particle size of colloids in natural systems (Lebron et al., 1993; Filella et al., 1997).

Field-Flow Fractionation

Field/flow fractionation (FFF) is a group of separation techniques capable of fractionating and characterizing the particle size distribution of colloids in the range 0.01 to 1 μm. Like chromatography, FFF is an elution methodology in which constituents are differentially retained, and thus separated in a flow channel (Beckett et al., 1997). With this technique, a colloidal sample is introduced into a stream of liquid and subjected to a field (such as gravitational, centrifugal, third crossflow, thermal gradient, electrical, or magnetic) acting perpendicular to the stream direction (Beckett and Hart, 1993). According to theory, the rate at which particles are displaced downstream, measured as emergence times, can be related exactly to particle properties such as mass, size, and density. However, since different kinds of particles move at different velocities in this system, broad particle populations are sorted into graded size (or mass) distributions along the length of the flow channel. Observation of the shape of the emerging distribution, combined with theory, yields particle size distribution curves.

If applied as indicated above, FFF provides highly detailed size distribution curves and is a highly flexible technique which can be adapted to different particle types in almost any suspending medium. Giddings et al. (1987) provide a detailed explanation of this technique.

Applications

Several instruments perform automated particle size analysis based on gravimetric sedimentation but differing in the method used to monitor the particle concentration. The more commonly used methods are X-ray and white light. At the beginning of the analysis the sample cell is positioned relative to a stationary detector at a depth sufficient to include the largest particles expected in the sample. The cell is then moved downward through the X-ray beam at a programmed rate. The time and depth in the suspension define a given particle diameter. The attenuation of the beam monitors the concentration of dispersed phase having this diameter. The results of the analysis are obtained as a graph of the cumulative mass percent as a function of the equivalent spherical diameter (Fig. 6.1).

The analytical application of PCS for size distribution measurements of natural colloidal suspensions provides valuable information about the system and it is one of the few nondestructive techniques that yields an estimate of the size distribution of suspended submicron colloids with a minimum of sample processing.

Precise information about colloidal size and shape is important because submicron size colloids often act as vehicles that govern the transport and fate of adsorbed pollutants (hydrophobic organic compounds, toxic trace metals and radionuclides). Submicron size colloids have been insufficiently studied because methods for their isolation, detection, and characterization have been inadequate except for a few examples (Kretzschmar et al., 1993; Kaplan et al., 1993). Little is known about

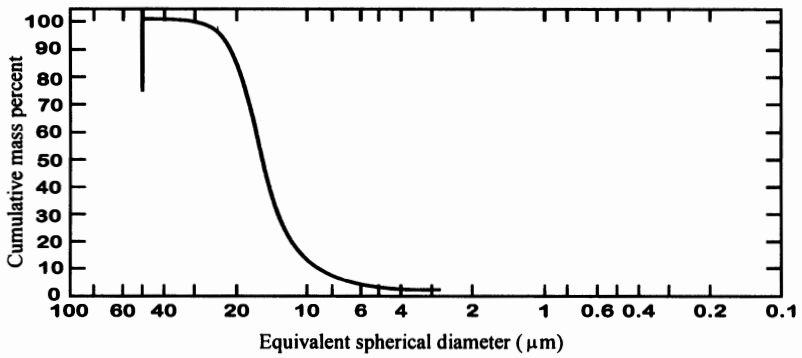

Fig. 6.1 Particle size distribution of glass spheres obtained using the Sedigraph 5000-D [Reprinted by permission of John Wiley & Sons, Inc. from Bunville, 1984. H.G. Barth (ed.) Modern methods of particle size analysis]

colloidal materials in natural environments, in particular, the chemical nature of colloids present and their structure, size and shape distributions (Filella et al., 1997).

The interpretation of many properties of clay suspensions has been traditionally based on a model of separated clay plates with well-developed electrical double layers. However, single plates of montmorillonite tend to assemble in an organized manner as quasicrystals. A group of aligned montmorillonite quasicrystals or illite crystals is described as a clay domain (Quirk and Aylmore, 1971). Schramm and Kwak (1982), using light transmission and viscosity measurements, found that quasicrystal size increased in the order of Li < Na < K < Mg < Ca. The average number of plates per quasicrystal relative to Li-montmorillonite varied from 1.5 for Na- to 6.1 for Ca-montmorillonite. Using PCS particle size analysis, Lebron et al. (1993) demonstrated the presence of illite domains in suspensions of sodium adsorption ratio [(SAR = $Na^+/(Ca^{2+}+Mg^{2+})^{0.5}$ where the cation concentration is expressed in mmol L^{-1})] < 15. Illite registered a decrease in the mean of the two dimensions of the domains (b and c crystal axis) when the SAR increased, while montmorillonite quasicrystal size decreased only in the c dimension. The b dimension of montmorillonite remained constant in the range of SAR studied. These differences are indicative of a different particle arrangement for illite domains than for montmorillonite quasicrystals (Fig. 6.2).

6.1.3.2 Surface Area

Surface area must be regarded as a relative term, in as much as it is scale dependent, as well as often dependent on the chemical and physical conditions in a system. Determinations of surface area range

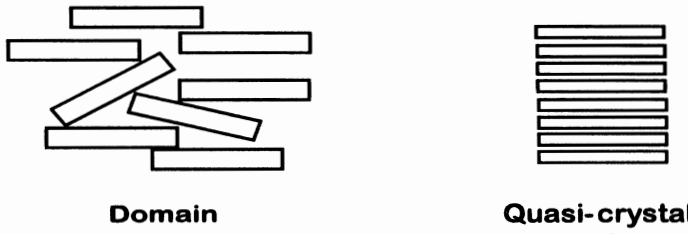

Fig. 6.2 Representation of mica domains and montmorillonite quasi-crystals based on photon correlation spectroscopy measurements [Reprinted from Lebron et al., 1993. Clays Clay Min. 41:380-388, with permission]

from particle size calculations assuming smooth surfaces and simplified geometry, generally termed geometric surface area, to possible molecular level calculations based on the distances between surface ions in a mineral structure. Because the measurement is scale and system dependent, there is no best way to measure surface area. Determination as to which measurement system to utilize should consider the scale and chemical conditions required by the application. Kinetic reactions which are diffusion controlled should likely consider geometric surface area while surface-controlled reactions (such as some adsorption and some dissolution/precipitation reactions) should consider surface area at the scale of the reacting molecule. In most instances, surface area is related to surface reactivity, either adsorption or surface-controlled kinetic processes.

Measurement Methodology

The results of surface area determinations must be interpreted within the context of the size and orientation of the adsorbate as well as the attractive forces between the surface and the adsorbate. This distinction is particularly important for clays such as smectites, which can be considered to have internal as well as external surface area. Internal surface area is representative of the surface area of the interlayers. Inert gases such as N_2 are not able to enter the interlayer positions, and thus, measure only external surface area of clay particles. In contrast, polar molecules such as ethylene glycol and water are able to cause expansion of the layers and penetrate into interlayer positions. Use of such molecules results in measurement of internal and external surface area. Since water is the solvent in environmental systems, these total surface area measurements are appropriate for adsorption studies.

To characterize adsorption methods of surface area determination, it is useful to distinguish between chemical and physical adsorption. Physical adsorption is characterized by: (1) low heats of adsorption without structural changes at the surface, (2) fully reversible and rapid reactions since no activation energy is required, (3) surface coverage of the entire surface rather than specific sites, (4) little or no adsorption at elevated temperatures, and (5) potential coverage by more than one layer of adsorbate (Lowell, 1979). Chemisorption is characterized by high heats of adsorption, localization of adsorption at specific surface sites, and irreversible reaction. The term specific surface area has been used to denote the surface area of a material expressed on a mass basis ($m^2\ kg^{-1}$).

Gas Adsorption Using the BET Equation

The BET equation is commonly used in conjunction with physical gas adsorption to measure surface area. The BET equation is named after Brunauer, Emmett, and Teller (1938), who extended the Langmuir theory for monolayer gas adsorption to multilayer adsorption. The Langmuir equation (Langmuir, 1918) is given by:

$$P / V = 1 / kV_m + P / V_m \qquad [6.11]$$

where P is the pressure, V is the volume of gas adsorbed per kg of adsorbent at that pressure, k is a constant, and V_m is the volume of gas adsorbed per kg of adsorbent at monolayer surface coverage. The surface area is obtained by determination of $1/ V_m$, which is the slope of the P/ V versus P plot. The specific surface area is then equal to $1/ V_m$ multiplied by the cross-sectional area of the adsorbate and the number of molecules in volume V_m.

The BET relation assumes that there is a dynamic equilibrium between the molecules in the various layers such that the number of molecules in each layer remains constant although different sites may or may not be occupied at any given time. Use of the equation enables calculation of the number of

molecules in a monolayer despite the fact that complete monolayer coverage may not have occurred. The BET equation is written as (Lowell, 1979):

$$\frac{1}{W[P_o / P]} = \frac{1}{W_m C} + \frac{C-1}{W_m C}\frac{P}{P_o} \quad [6.12]$$

where P is the adsorbate gas pressure, P_o is the adsorbate pressure at saturation for the temperature of the experiment, W is the weight adsorbed in the monolayer, W_m is the weight adsorbed in the complete monolayer, and C is the BET constant. Multipoint BET plots are created by plotting $1/(W(P_o/P-1))$ on the y axis and P/P_o on the x axis. The value of W_m is calculated from the slope and intercept. The specific surface area is determined by dividing the total surface area by the sample weight. The region of P/P_0 between 0.05 and 0.35 is usually linear and within the region of pressures corresponding to sufficient adsorption to complete monolayer coverage, and thus, best suited for determination of W_m (Lowell, 1979).

Often the BET surface area can be determined from a single pressure measurement without much loss of accuracy. For relatively high values of C, the intercept value is small relative to the slope and can be approximated by zero. The BET equation is thus reduced to (Lowell, 1979):

$$W_m = W\left(1 - \frac{P}{P_o}\right) \quad [6.13]$$

Soil and mineral surface areas are most commonly measured by N_2 sorption using the BET equation. The calculation is made using the N_2 cross-sectional area of 0.162 nm^2 (Gregg and Sing, 1982). Often, this area is referred to as the effective or occupied area. Alternatively for surface area < 1,000 $m^2\ kg^{-1}$, the use of Kr is recommended.

Most commonly, the BET method consists of adsorption of N_2 at a fixed partial pressure P in a He-N_2 mixture and measurement of the desorbed N_2 in a pure He gas stream using gas chromatography. Alternative methods include measurement of the mass of N_2 sorbed. In this method, the sample is evacuated to high vacuum, heated, then cooled to liquid N_2 temperature and weighed. Quantities of N_2 are then added to the system and a series of weighings is made at various pressures. In this instance, the N_2 partial pressures are equal to the total pressure in the system.

Organic Molecules

Ethylene Glycol. Ethylene glycol was utilized by Dyal and Hendricks (1950) for determination of the total surface area of clays. The method consists of adding excess of ethylene glycol to soil or clays and allowing the excess to evaporate under vacuum. It is assumed that when the rate of weight loss of the sample decreases only a monolayer of ethylene glycol remains. Dyal and Hendricks (1950) calibrated the method assuming a bentonite surface area of 810,000 $m^2\ kg^{-1}$ and calculated that 0.31 mg of adsorbed ethylene glycol corresponded to each m^2 of surface area. The method was modified by Bower and Goertzen (1959) by using $CaCl_2$-monoglycolate to maintain an ethylene glycol vapor pressure just below that of the saturation vapor pressure. In this method the sample and the liquid are placed in separate open vessels in an evacuated system and the sample is weighed until it is in equilibrium with the vapor pressure of the ethylene glycol.

Ethylene Glycol Monoethyl Ether. Ethylene glycol monoethyl ether (EGME) has replaced ethylene glycol as the polar solvent of choice for determination of surface area. Since EGME has a higher vapor pressure than ethylene glycol, it requires a shorter reaction time to equilibrate the sample (Carter et al., 1986). A solvate of EGME and $CaCl_2$ is used in the evacuated chamber to lower the vapor pressure of EGME to just below the saturation pressure. Open vessels of EGME/$CaCl_2$ and soil are placed in the chamber and the soil is periodically weighed until no further weight gain is observed. It is assumed that the EGME surface coverage is 5.2×10^{-19} m^2 per molecule and that 0.286 mg adsorbed corresponds to one m^2 of surface area (Carter et al., 1986). The method is limited in that the EGME affinity for cations results in greater than monolayer coverage at those sites, the assumption that EGME covers all surfaces cannot be properly evaluated, and the large size of the molecule may prevent coverage in small surface voids.

Methylene Blue. Methylene blue, an organic cation, is reacted at various concentrations with soil suspensions (typically with organic material removed) under pH buffered conditions. Measurement of methylene blue concentration before and after reaction with soil is made using spectrophotometry at a wavelength of 665 nm. The adsorbed concentration of methylene blue is used to calculate surface area assuming an area of 1.3 nm^2 per methylene blue molecule (Pham and Brindley, 1970). This surface area corresponds to the molecule attaching parallel to its long axis. This method can only be used in hydrated systems. Alternatively, Borkovec et al. (1993) obtained relatively good agreement between methylene blue and BET surface areas for 4 soil samples assuming a methylene blue surface area of 0.247 nm^2, corresponding to a molecular attachment of methylene blue perpendicular to its long axis. Orientation of the organic molecules may be related to surface site characteristics as well as concentration of adsorbing molecules. These differences illustrate one of the disadvantages of using charged molecules for surface area determination; their use is not recommended.

Scanning Electron Microscopy Image Analysis

Transmission (TEM) as well as scanning electron microscopy (SEM) can be used for determination of geometric surface area using a variety of methods, including calculation of planar surface area and assumptions regarding geometry to calculate total external surface area. With this method, only edge roughness can be measured. The SEM method, which offers the possibility of measuring the external surface roughness, consists of collecting two images at different sample tilt angles and constructing a 3-dimensional representation of the surface. Surface area is calculated within a grid of fixed lines by summation of the planar surfaces in the grid. The ratio of the calculated surface to the area within the grid gives a measure of surface roughness. Measurements can also be made at different scales, providing information about the size distribution of the surface features. Since these measurements are typically made at the micrometer scale and measure external surface area, it is not surprising that the values are intermediate between geometric surface areas based on particle size and BET values. Determination of specific surface area requires conversion of particle surface area to a mass basis using the particle density. The assumption that particle density is equal to density of specimen samples of the mineral is reasonable and introduces relatively minor errors in comparison to other assumptions made in the calculation. The advent of large computer storage devices and suitable software makes this method the most useful of the geometric methods.

Small Angle X-ray Scattering

In this application, $K\alpha$ radiation from a conventional X-ray tube is scattered by freeze-dried samples in glass capillary tubes. The background corrected X-ray scattering intensity is plotted against the

scattering vector (q) to obtain the apparent surface fractal dimension (D_s) using the relation (Borkovec et al., 1993):

$$I_q = Aq^{D_s-5} + B \quad [6.14]$$

where I_q is the scattering intensity, A is a proportionality constant, and B is the background correction. Values of D_s obtained for soils using this method are in relatively good agreement with values calculated from gas adsorption surface area (a) for soil particle radii (r) using the relation (Borkovec, 1993):

$$a = C\lambda^{2-D_s} r^{D_s-3} \quad [6.15]$$

where λ is the size of the probing molecules and C is the proportionality constant.

Negative Adsorption

Negative adsorption refers to a deficiency in the concentration of an ion in solution adjacent to a solid surface relative to the concentration of the ion in the bulk solution. The deficit is caused by electrostatic repulsion between ions and surfaces of similar charge. Since most charged surfaces in soils are negatively charged, negative adsorption usually relates to solution anion concentrations and negative surfaces. For a 1:1 electrolyte, the diffuse double layer model produces the following approximation (Sposito, 1984):

$$d_e \approx \frac{2}{\sqrt{\beta c}} - \delta \quad [6.16]$$

where d_e is the exclusion distance, c is the concentration of the bulk electrolyte, ß is a constant equal to 1.08×10^{16} $m.mol^{-1}$, and δ is the distance between two planes. The exclusion volume and area (S_e) are related by:

$$V_e = S_e d_e \quad [6.17]$$

where V_e is the exclusion volume (the hypothetical volume from which the ion is completely excluded). Substituting into Equation [16] yields:

$$V_e = \frac{2S_e}{\sqrt{\beta c}} - \delta S_e \quad [6.18]$$

The exclusion volume is calculated by first removing the bulk solution, determining the remaining liquid volume, displacing the liquid and analyzing for the bulk solution and extract concentration. The exclusion volume is then equal to the mass deficit in the extract divided by the concentration in the bulk solution. A plot of V_e versus $c^{-0.5}$ should yield a straight line whose slope is proportional to the exclusion specific surface area as shown by inspection of Equation [6.18].

This method was first described by Schofield (1949) who used it to determine montmorillonite surface area from reactions with NaCl, $NaNO_3$, and Na_2SO_4 solutions. Subsequent work by Edwards

et al. (1965a,b) demonstrated that the specific area determined with this method varied with cation selected. Calculated values for illites ranged in values close to the BET values with Li to 0 with Cs. In contrast, for montmorillonite, LiCl exclusion values were ten times greater than BET, while Cs values were comparable to those obtained by BET.

Applications

Surface area measurements are required for a variety of calculations. In most soils the bulk soil surface area is dominated by the surface area of the clay minerals. Surface charge density, which requires measurement of both surface area and particle charge, has been related to cation exchange selectivity. As expected, increasing surface charge density favors adsorption of the higher valence cation in heterovalent exchange (Maes and Cremers, 1977). Determination of specific surface area is required for chemical studies on many different minerals. In this case, bulk surface area is not appropriate. Controlled laboratory studies are often performed using addition of quantities of a well-characterized mineral having a known surface area. This method is used to study a variety of chemical reactions, such as kinetics of calcite, gypsum, and dolomite dissolution, surface area of calcite for prediction of phosphate adsorption, and addition of various Fe or Mn oxides for study of adsorption and redox processes. Among the various applications of the EGME method, Ross (1978) related shrink/swell properties of soils to surface area and Supak et al. (1978) related the specific surface area of clays to the adsorption of the pesticide aldicarb.

6.1.3.3 Surface Charge

The total net surface charge on a particle (σ_p) is

$$\sigma_p = \sigma_s + \sigma_H + \sigma_{is} = \sigma_{os} - \sigma_d \qquad [6.19]$$

where σ_s is the permanent structural charge, σ_H is the proton surface charge resulting from the specific adsorption of protons and hydroxyl ions, σ_{is} is the inner-sphere complex charge resulting from specific ion adsorption, σ_{os} is the outer-sphere complex charge resulting from nonspecific adsorption, and σ_d is the dissociated charge. This definition is similar to the one provided by Sposito (1984) with the exception that total net surface charge results from isomorphic substitution and is generated by specifically adsorbing ions (Hunter, 1981). Inner- and outer-sphere surface complexes differ in containing no water (inner) and at least one water molecule (outer) between the adsorbing ion and the surface functional group (Sposito, 1984). Examples of surface functional groups are reactive surface hydroxyl groups on oxide minerals, aluminol and silanol groups on clay minerals, and carboxyl and phenol groups on SOM.

Measurement Methodology

The total net surface charge can be measured directly using electrokinetic experiments. The point of zero charge (p.z.c.) of a particle is the solution pH value where total net particle charge is zero. The p.z.c. can be measured directly using electrokinetic experiments or indirectly from potentiometric titrations under certain experimental conditions (Sposito, 1984).

Electrokinetic phenomena are processes where a relative velocity exists between two parts of the electrical double layer (Hiemenz, 1977). In this motion, a thin layer of liquid remains with the solid and a shear plane is located between the solid and liquid phases at some distance from the solid surface (van Olphen, 1977). The electric double layer potential at the shear plane is called the zeta potential (ζ). The assumption that ζ is equal to or very close to the diffuse double layer potential (ψ_d)

is supported indirectly by a large body of data on a variety of surfaces (Hunter, 1981, 1989). The principal electrokinetic phenomena that measure ζ potential are discussed below.

Electrophoresis

Electrophoresis measures the movement of a suspended charged particle in response to an applied electric field. This movement is called electrophoretic mobility (u_E) and is given by the Smoluchowski equation (Hunter, 1989):

$$u_E = \frac{\varepsilon\zeta}{\eta} \qquad [6.20]$$

where ε is the relative permittivity and η is the viscosity. The Smoluchowski equation applies when the particle dimensions are much greater than the double layer thickness (Hunter, 1987). The complete formula relating ζ and u_E is derived by the theoretical evaluation of the electric force on the charged particle (f_1), the hydrodynamic frictional force on the particle by the liquid (f_2), the electrophoretic retardation force (f_3), a frictional force resulting from the movement of water with the counter ions, and the relaxation force (f_4), caused by distortion of the double layer around the particle (van Olphen, 1977). Additional considerations arise for nonspherical particles and those carrying two double layers such as clays. For these reasons, the Smoluchowski equation is, in general, only approximate and it is advisable to report electrophoresis results as electrophoretic mobility rather than attempt to convert to ζ potential (van Olphen, 1977).

Electrophoresis is the most common method of determining ζ potential. For colloidal systems the most important technique is microelectrophoresis where the movement of individual particles is followed directly by microscopy (Hunter, 1981). Microelectrophoresis is only applicable at very low particle concentrations. Electrophoresis can also be studied using laser Doppler velocimetry and photon correlation spectroscopy. The mass transport mobility apparatus measures electrophoretic mobility from the mass of colloids transported to a suitable electrode compartment (Hunter, 1981). This apparatus can be used at much higher particle concentrations than microelectrophoresis.

Electroosmosis

Electroosmosis measures the movement of the liquid adjacent to a flat, charged surface in response to an electric field applied parallel to the surface. This movement is called electroosmotic velocity (v_{eo}) and is also obtained from the Smoluchowski equation (Hunter, 1987):

$$v_{eo} = \frac{-\varepsilon\zeta}{\eta} \qquad [6.21]$$

where E is the electric field strength. While it is possible to measure electroosmotic velocity directly using microscopy, it is more common to measure the volume of liquid transported per unit time (Hunter, 1981):

$$\frac{V}{i} = \frac{\varepsilon\zeta}{\eta\lambda_0} \qquad [6.22]$$

where V is volume, i is the electric current and λ_0 is the electrical conductivity. The material whose ζ potential is being measured is formed into a porous plug and the transport of liquid across a tube in response to an electric field may be obtained by measuring the movement of an air bubble in the capillary providing the return path (Adamson, 1976). It is also possible to measure the electroosmotic flow by applying a counter pressure until the flow is exactly compensated (Hunter, 1981).

Streaming Potential

The streaming potential is an electric potential difference generated when liquid adjacent to a charged surface is set in motion by an applied pressure gradient (Hunter, 1987). The streaming potential (Φ_{st}) is also governed by the Smoluchowski equation and given by (Sposito, 1984):

$$\Phi_{st} = \frac{\varepsilon\zeta}{\lambda_0 \eta}\Delta P \qquad [6.23]$$

where ΔP is the applied pressure difference. The streaming potential can be measured in similar fashion as the electroosmotic velocity. Liquid is forced under pressure through a porous plug and Φ_{st} is measured by electrodes in the solution on either end (Adamson, 1976).

Sedimentation Potential

When particles having charged surfaces sediment in a liquid under the force of gravity, a plane of shear is developed. As the particles settle, the interfacial charge is separated since a portion inside the shear plane moves with the particle and the remainder is left behind (Sposito, 1984). An electric potential difference arises from the separation of charge called the sedimentation potential. The gradient for the sedimentation potential ($d\Phi_{sed}$) is given by (Sposito, 1984):

$$\frac{d\Phi_{sed}}{dz} = \frac{\varepsilon\zeta}{\lambda_0 \eta} n\Delta\rho g \qquad [6.24]$$

where n is the number of particles per unit volume, $\Delta\rho$ is the difference in mass density between the particles and the liquid phase, g is gravitational acceleration and z is distance. The potential difference is measured by inserting reversible electrode probes at two different heights in the column of settling particles (Hunter, 1981). For low particle concentration the sedimentation potential is also governed by the Smoluchowski equation (Hunter, 1981).

Potentiometric Titration

Potentiometric titration measures the surface density of proton surface charge (σ_H) defined as (Sposito, 1984):

$$\sigma_H = \frac{F}{A}(q_H - q_{OH}) \qquad [6.25]$$

where F is the Faraday constant, A is specific surface area, q_H is the complexed proton charge (moles), and q_{OH} is the complexed hydroxyl charge (moles) per unit mass of solid. Titration data consist of pH readings obtained while known amounts of acid or base are added to a solid suspension. A net titration

curve is obtained by subtracting a calibration curve obtained by titrating the equivalent supernatant solution. The values of $(q_H - q_{OH})$ are given by (Sposito, 1984):

$$q_H - q_{OH} = \frac{C_A - C_B - [H^+] + [OH^-]}{C_s} \qquad [6.26]$$

where C_A is the molar concentration of acid added, C_B is the molar concentration of base added, $[H^+]$ is the molar proton concentration and $[OH^-]$ is the molar hydroxyl concentration obtained from pH measurement, and C_s is the particle concentration. In order for Equation [6.26] to be valid, added protons and hydroxyl ions must only react with variable charge surface reactive groups. Usually, other reactions occur which are also pH dependent such as soluble complex formation, dissolution of solid phases, or complexation with surfaces whose charge is not variable (Parker, 1979). Thus without these corrections no surface chemical significance can be provided by Equation [6.26]. A detailed

Table 6.3 Representative points of zero charge for various minerals

Solid	p.z.c.
	Electrophoresis
Goethite	8.8
Hematite	8.5
Magnetite	6.9
Amorphous iron oxide	8.0
Gibbsite	9.8
Bayerite	9.2
Boehmite	9.4
Pseudoboehmite	9.2
Amorphous aluminum oxide	9.3
δ-MnO_2	2.3
Rutile	4.8
Anatase	5.9
Kaolinite	2.9
	Streaming Potential
γ-Al_2O_3	9.1
α-Al_2O_3	9.2
	Titration
Goethite	8.7
Hematite	8.6
Magnetite	6.9
Gibbsite	9.8
Boehmite	8.5
Pseudoboehmite	9.3
Amorphous aluminum oxide	9.5
δ-MnO_2	3.6
SiO_2	3.0
Rutile	5.8
Anatase	6.0
Kaolinite	2.9

description of the use of potentiometric titration to determine surface charge is provided by Huang (1981).

Applications

One of the most important applications of electrokinetic experiments and potentiometric titrations is the determination of the p.z.c. A characteristic of variable charge minerals is the p.z.c. obtained in the presence of an inert electrolyte. This p.z.c. is determined electrokinetically as the pH value where the ζ potential is zero or indirectly from the point of zero net proton charge (p.z.n.p.c) or from the point of zero salt effect (p.z.s.e.) obtained potentiometrically. The p.z.n.p.c and the p.z.s.e. are discussed in Section B, Chapter 7. The p.z.n.p.c and the p.z.s.e. are equivalent to the p.z.c. in the absence of surface complex formation. Table 6.3 provides characteristic values of p.z.c. obtained using electrokinetic experiments and potentiometric titrations for a variety of variable charge minerals.

Electrokinetic experiments and potentiometric titrations can be used to infer adsorption mechanisms for adsorbing ions on surfaces. Adsorption of ions that form inner-sphere surface complexes is characterized by shifts in the p.z.c of the particles and reversals of their electrophoretic mobility with increasing ion concentration (Hunter, 1981). Adsorption of ions that form outer-sphere surface complexes does not produce p.z.c. shifts since they are assumed to lie outside the shear plane. Fig. 6.3 presents the shifts in p.z.c. and charge reversals observed for gibbsite upon the specific adsorption of increasing amounts of molybdate. These results are indirect evidence for inner-sphere surface complexation of this ion.

Net particle surface charge is a primary factor in dispersion of clay minerals. Zeta potential as a measure of particle surface charge was also related to percentage of dispersible clay (Chorom and Rengasamy, 1995). Fig. 6.4 indicates the relationship between ζ potential measured using electrophoresis, and dispersible clay for Na saturated kaolinite, montmorillonite, and illite.

The plane interface technique determines the electroosmotic velocity at large plane interfaces and can be used to determine the ζ potential of two different surfaces at the same time under the same conditions (Nishimura et al., 1992). These authors used the plane interface technique to simultaneously study silica plates and muscovite mica basal planes. The ζ potential values for silica presented in Fig. 6.5 indicate that the asymmetric silica-mica cell provides results comparable to those of the symmetrical silica-silica cell.

Zeta potentials of muscovite mica have also been determined using a flat plate streaming potential apparatus (Scales et al., 1990). Zeta potential of clays becomes less negative with increasing

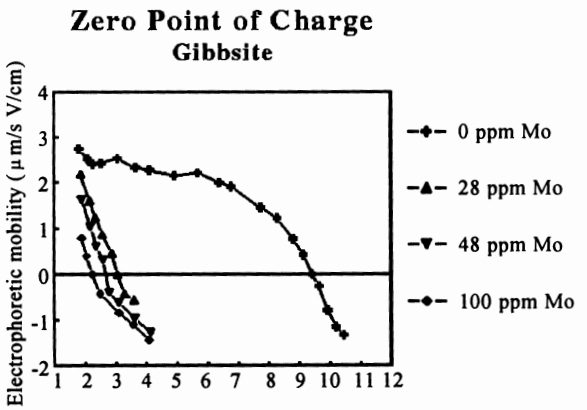

Fig. 6.3 Shifts in p.z.c. and charge reversal of gibbsite in the presence of molybdate [From Goldberg et al., 1996]

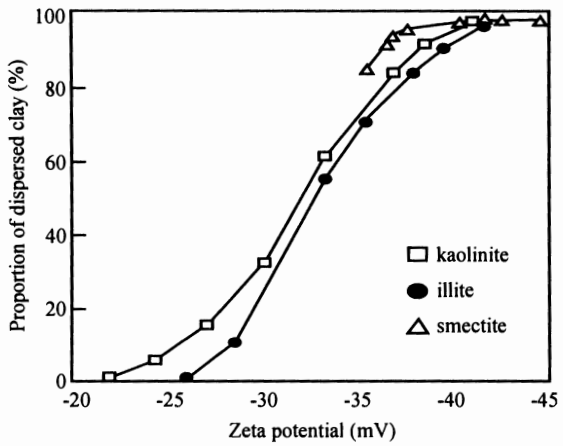

Fig. 6.4 Relation between zeta potential and dispersible clay of Na-clay minerals obtained using electrophoresis [Reprinted by permission of Blackwell Science Ltd, Oxford, UK from Chorom and Rengasamy, 1995. Europ. J. Soil Sci. 46:657-665]

electrolyte concentration as a result of double layer compression (Fig. 6.6). The resulting charge reduction causes clay flocculation.

A vastly different application of electrokinetic experiments is the application to dewatering and decontamination of soils and clays. For example, electroosmosis has been used for removing organic contaminants from kaolinite clays (Shapiro and Probstein, 1993). These authors present an application for *in situ* hazardous waste remediation of soil.

A potentiometric titration method has been developed to account for changes in solubility of the solid with changes in pH (Schulthess and Sparks, 1986). This is a batch method where the reference for each sample is the supernatant specific to that sample backtitrated to pH 7. This method is considered to account for all sources of proton consumption (Schulthess and Sparks, 1986).

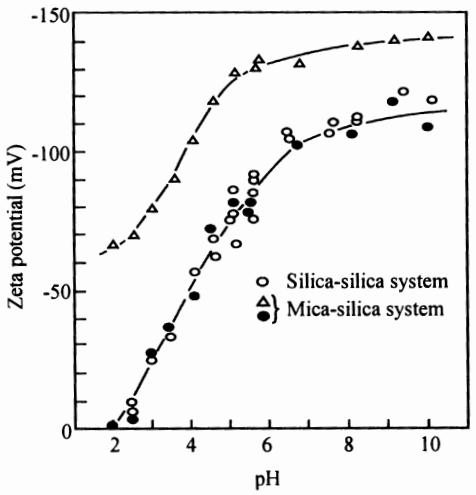

Fig. 6.5 Zeta potentials as a function of solution pH for muscovite mica basal plane-and silica plate-aqueous solution interfaces obtained using electroosmosis [Reprinted by permission of Academic Press, Inc. from Nishimura et al., 1992. J. Colloid Interf. Sci. 152:359-367]

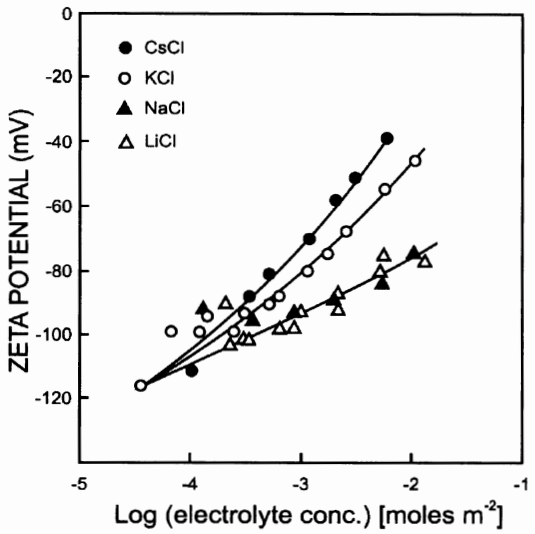

Fig. 6.6 Relation between zeta potential and electrolyte concentration for various 1:1 electrolytes obtained from streaming potential [Reprinted from Scales et al., 1990. Langmuir 6:582-589. Copyright American Chemical Society]

6.1.4 Thermodynamics of Colloid Surfaces

To develop the thermodynamic treatment of the surface region, a few definitions are useful. The interfacial region is a space between two adjoining phases (gas-liquid, gas-solid, liquid-liquid, liquid-solid, solid-solid) which is characterized by inhomogeneity in its properties. The Gibbs surface is a mathematical dividing surface, without volume, drawn parallel to the boundaries of the interfacial region, which is used to define the volumes of the two adjoining bulk phases. A schematic of the interfacial region and the Gibbs surface is presented in Fig. 6.7. The actual values for the system as a whole will differ from the sum of the values for the bulk phases by an excess or deficiency due to the Gibbs surface (Adamson, 1976). The following relations hold for the variables of state:

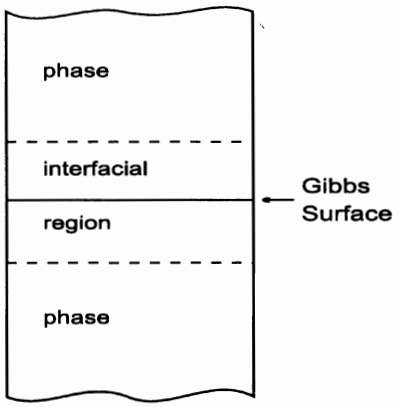

Fig. 6.7 Representation of the interface region and the Gibbs surface

$$\begin{aligned} \text{Volume:} \quad & V = V^{\alpha} - V^{\beta} \\ \text{Internal Energy:} \quad & E = E^{\alpha} + E^{\beta} + E^{\sigma} \\ \text{Entropy:} \quad & S = S^{\alpha} + S^{\beta} + S^{\sigma} \\ \text{Moles:} \quad & n_i = n_i^{\alpha} + n_i^{\beta} + n_i^{\sigma} \end{aligned} \qquad [6.27]$$

where α and ß denote the bulk phases and σ denotes the Gibbs surface (Adamson, 1976). Additional variables of state are defined as the surface tension or surface free energy (γ) and the area of the Gibbs surface (A).

The three fundamental thermodynamic relationships of surface chemistry are the Young-Laplace equation, the Kelvin equation, and the Gibbs equation (Adamson, 1976). The Young-Laplace equation is the fundamental equation of capillarity for a curved Gibbs surface:

$$P^{\beta} - P^{\alpha} = \gamma\left(\frac{1}{r_1} + \frac{1}{r_2}\right) \qquad [6.28]$$

where $(P^{\beta} - P^{\alpha})$ is the capillary pressure and r_1 and r_2 are the radii of curvature.

The Kelvin equation gives the effect of surface curvature on the molar free energy of a substance. The free energy of a substance can be related to its vapor pressure assuming the vapor to be ideal (Adamson, 1976). The Kelvin equation is

$$\ln\left(\frac{P}{P^0}\right) = \frac{\gamma V}{RT}\left(\frac{1}{r_1} + \frac{1}{r_2}\right) \qquad [6.29]$$

where P^0 is the normal vapor pressure of the liquid, P is the vapor pressure observed over the curved surface, and R is the molar gas constant, and T is temperature.

For a small, reversible change dE in the energy of the system (Adamson, 1976):

$$\begin{aligned} dE = dE^{\alpha} + dE^{\beta} + dE^{\sigma} = TdS^{\alpha} + \sum \mu_i dn_i^{\alpha} - P^{\alpha}dV^{\alpha} + TdS^{\beta} \\ + \sum \mu_i dn_i^{\beta} - P^{\beta}dV^{\beta} + TdS^{\sigma} + \sum \mu_i dn_i^{\sigma} - P^{\sigma}dV^{\sigma} + \gamma dA \end{aligned} \qquad [6.30]$$

where μ_i is chemical potential. Substituting for dE^{α} and dE^{β} and manipulating the equation for dE^{σ} lead to the expression (Adamson, 1976):

$$S^{\alpha}dT = Ad\gamma + \sum n_i^{\sigma} d\mu_i = 0 \qquad [6.31]$$

At constant T and A, the Gibbs equation is

$$-d\gamma = \sum \frac{n_i^{\sigma}}{A} d\mu_i = \sum \Gamma_i^{\sigma} d\mu_i \qquad [6.32]$$

where Γ_i^σ is a surface excess concentration per unit area defined as $\Gamma_i^\sigma = n_i^\sigma/A$. The Gibbs equation can be applied to liquid-liquid and liquid-vapor interfaces where the surface tension can be measured to calculate the surface concentration of the adsorbed species causing the surface tension change. Similarly, if the surface concentration can be measured directly but the surface tension cannot, the Gibbs equation can be used to calculate the lowering of γ from the measured adsorption in solid-gas and solid-liquid systems (Hunter, 1987).

6.2 Interparticle Forces

6.2.1 Electrical Double Layer

Double layer theory describes the distribution of ionic concentrations near electrostatically charged particles. The charge on the colloidal particles is due to isomorphic substitution in the particle lattices or arises from the preferential adsorption of one ionic species from the solution phase (Babcock, 1963). Such a charge requires the presence of a layer of ions of opposite charge. The double layer consists of an excess of ions of opposite sign and a deficiency of ions of the same sign that are electrostatically repelled by the particle. Double layer theory assumes that the surface of the colloidal particles is represented by an infinite flat surface having continuous and uniform electrostatic charge density immersed in an electrolyte with a uniform dielectric constant (Babcock, 1963). All electrolyte ions are assumed to be point charges. The electrical potential, ion charge, and ion distributions can be calculated from the Poisson-Boltzmann equation:

$$\frac{d^2\psi}{dx^2} = -\frac{1}{\varepsilon_0 D}\sum cFz_i \exp\left(-z_i F\psi(x)/RT\right) \qquad [6.33]$$

where $\psi(x)$ is the inner potential at a distance x from the surface, e_0 is the permittivity of free space, D is the dielectric constant of water, c is the concentration, R is the gas constant, T is the temperature (K), F is the Faraday constant, and z_i is the valence of the charged species (Sposito, 1984). Figs. 6.8 and 6.9 present the ion distribution and the electric potential distribution, respectively, in the double

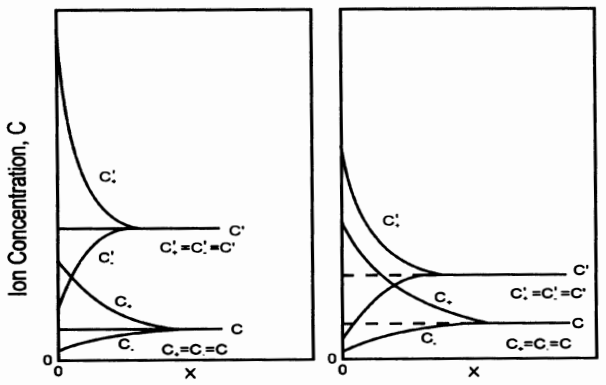

Fig 6.8 Distribution of ions in the electric double layer at two electrolyte concentrations (c' > c). Left: constant potential surface. Right: constant surface charge [Adapted from van Olphen, 1977. An introduction to clay colloid chemistry. Copyright John Wiley & Sons, New York with permission]

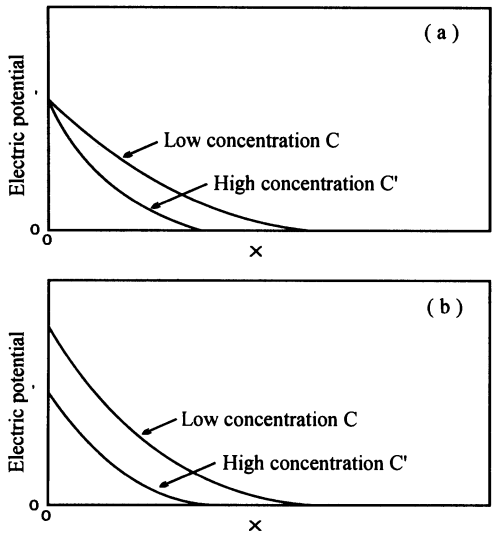

Fig. 6.9 Electrical potential distribution in the double layer at two electrolyte concentrations. Top: constant potential surface. Bottom: constant surface charge [Adapted from van Olphen, 1977. An introduction to clay colloid chemistry. Copyright John Wiley and Sons, New York with permssion]

layer at two electrolyte concentrations. The extent of the double layer is given by the distance ($1/\kappa$) in units of m:

$$\frac{1}{\kappa} = \sqrt{\frac{\varepsilon_0 RT}{2000F^2 I}} \qquad [6.34]$$

where I is the ionic strength ($=^1/_2 \Sigma\, c_i\, z_i^2$). Important findings of diffuse double layer theory are (1) the excess cations near the negative surface neutralize more of the charge than the anion deficit; (2) the electric potential decreases as the electrolyte concentration increases; (3) the double layer distance ($1/\kappa$) decreases as the electrolyte concentration increases. Some important limitations of double layer theory are that it applies only to infinitely dilute suspensions and to low surface charge densities (Babcock, 1963).

6.2.2 Attractive Force

The attractive force acting on colloidal particles is called the van der Waals force and acts to bring particles closer together. The basis of the attractive force is that the fluctuating dipole of one atom polarizes another and the two atoms attract each other. This attraction between atom pairs is additive, and therefore, the energy of interaction between particles decreases much more slowly with distance than that between individual atoms (Quirk, 1994). The interaction energy per unit area between two opposing planar solids for the van der Waals force (Φ_{vdW}) is (Israelachvili, 1992):

$$\Phi_{vdW} = -\frac{A_H}{12\pi d^2} \qquad [6.35]$$

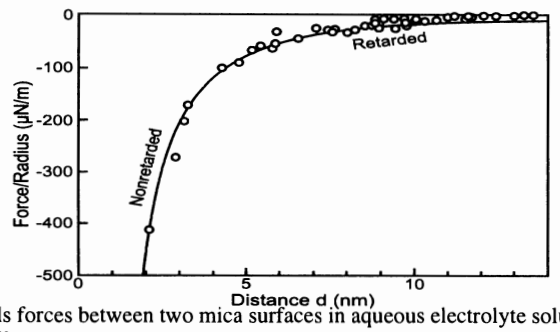

Fig. 6.10 van der Waals forces between two mica surfaces in aqueous electrolyte solutions. The measured Hamaker constant is A = 2.2×10^{-20} J. Retarded van der Waals forces are observed above 5 nm [Reprinted from Israelachvili, 1992. Intermolecular and surfaces forces. Academic Press Ltd, London, UK with permission].

where A_H is the Hamaker constant and d is the distance separating the solid surfaces. At distances > 5 nm, the correlations between the induced dipole distributions weaken and the interaction energy per unit area corresponds to the retarded van der Waals force (Φ_{RvdW}):

$$\Phi_{RvdW} = -\frac{B_{rH}}{3d^3} \qquad [6.36]$$

where B_{rH} is the retarded Hamaker constant. Fig. 6.10 shows values of the van der Waals force obtained experimentally between two mica surfaces.

6.2.3 Repulsive Force

The electrostatic force results from the charge on the colloidal particles and acts to repel them. A force operates on charged surfaces as a result of their interacting double layers. This force is repulsive if the charges on the particles are the same. The repulsion described in terms of interaction energy per unit area (Φ_R) is given by the force times the distance through which it operates (Hiemenz, 1977):

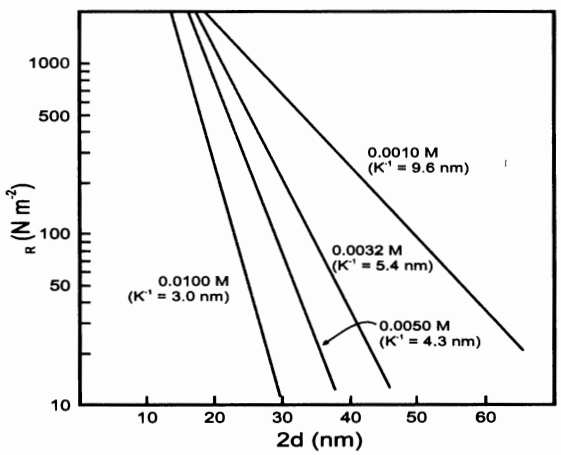

Fig. 6.11 Repulsive force between two plates for different concentrations of a 1:1 electrolyte where K is the inverse double layer distance [Reprinted by permission of Marcel Dekker, Inc. from Hiemenz, 1977. Principles of colloid and surface chemistry]

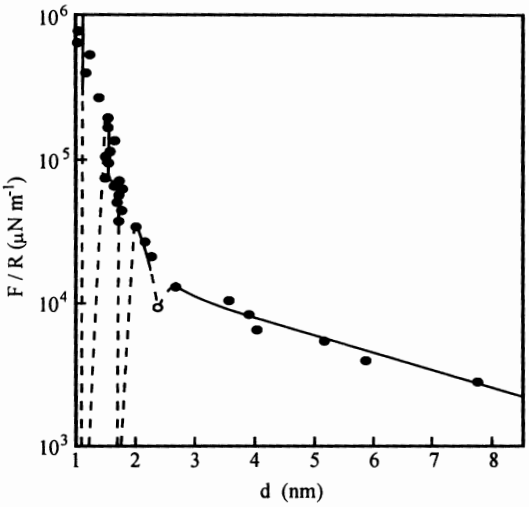

Fig. 6.12 Forces between two mica surfaces in 7 mmol L^{-1} NaCl electrolyte. F is the total force scaled by the radius (R) of the curved surfaces. At distance > 1.5 nm, the forces are described by double layer theory. Hydration forces are observed at distances < 1.5 nm [Reprinted with permission from Ducker and Pashley, 1992. Langmuir 8:109-112. Copyright American Chemical Society].

$$\Phi_R = -\frac{64a^2}{z} cRT \exp(-z\kappa d) \qquad [6.37]$$

where $a = \tanh(z\psi_0/4RT)$, z is the charge on the electrolyte ions, c is the concentration of the electrolyte ions, κ is the inverse double layer distance, and d is ½ of the surface separation.. This equation is valid only when the surface separation $2d \gg 1/\kappa$ and $a \approx 1$. The electrostatic force between two plates for different electrolyte concentrations is presented in Fig. 6.11.

When surfaces are brought closer and closer together or, when water is the medium (hydration force), an additional repulsive force (solvation force) becomes important. Solvation forces are short range and oscillatory and arise whenever liquid molecules are induced to order between surfaces. Between colloid surfaces, repulsive hydration forces arise when water molecules strongly bind to hydrogen bonding surface groups such as hydrated ions or hydroxyl groups (Israelachvili, 1992). The effective range of hydration forces in clays and silicates is 3–5 nm. The interaction of mica surfaces in dilute solution obeys double layer theory, but at higher electrolyte concentration, a hydration force develops due to the energy needed to dehydrate surface bound cations. The strength of the hydration force which increases with the hydration number of the cation $Mg^{2+} > Ca^{2+} > Li^+ \approx Na^+ > K^+ > Cs^+$ (Israelachvili, 1992) is illustrated for two mica surfaces in Fig. 6.12.

Clay swelling is the result of double layer repulsion between the surfaces of individual particles. Under confining conditions, a fluid pressure or swelling pressure is created that is a direct measure of the balance of forces between particles (van Olphen, 1977). The swelling pressure is obtained by measuring the confining force that must be applied to keep the clay layers at a given distance. The swelling pressure (Π) is

$$\Pi = P_{vdW} + P_R \qquad [6.38]$$

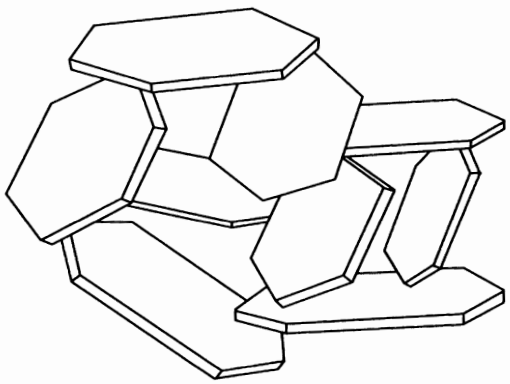

Fig. 6.13 Representation of card house structure [Reprinted by permission of Oxford University Press from Hunter, 1987. Foundations of colloid science Vol. 1]

where P_{vdW} is the van der Waals force and P_R is the electrostatic force (Greathouse et al., 1994). At short distances, hydration forces become significant in the swelling pressure. At greater distances, measured swelling pressures are of similar magnitude to calculated double layer repulsions (van Olphen, 1977).

Interparticle forces can be measured experimentally using the surface force apparatus (SFA), total internal reflectance microscopy, and the atomic force microscope (AFM) (Israelachvili, 1992). The SFA has been used to measure attractive van der Waals forces, repulsive double layer forces, and repulsive hydration forces in aqueous solutions at the 10^{-10} m level of resolution (Israelachvili, 1992). Because of its smooth surface and ease of handling, mica has been the primary solid used in SFA studies. Total internal reflection microscopy has been used to study forces between a surface and an individual colloidal particle. Atomic force microscopy has been used to measure both short- and long-range forces. Interactions between charged mica surfaces have been investigated using a combination of SFA and AFM experiments. Results from both methods agree with theoretical predictions (Kékicheff et al., 1993).

6.3 Colloidal Stability

6.3.1 Flocculation and Dispersion

The stability of colloidal suspensions is a balance between repulsive and attractive forces acting among the suspended particles. If net repulsive forces predominate, particles do not coagulate and they remain dispersed. When the attractive forces are dominant, interacting particles coagulate and the resulting floccules settle more rapidly from the suspension than the smaller dispersed particles. This theory is referred to as DLVO after Derjaguin, Landau, Verwey, and Overbeek who were largely responsible for its development (Hunter, 1987).

Flocculation is a thermodynamically favorable process; however, the kinetics of coagulation determine the stability of colloidal suspensions. Generally, all colloidal suspensions will spontaneously flocculate given sufficient time, but potential energy barriers retard the rate of flocculation. These barriers are analogous to activation energies considered in chemical kinetics (Hiemenz, 1977). Particles in a primary minimum are adhesive and are not readily separated. In contrast the dispersion/

flocculation transition is the result of a secondary minimum, involves card house type structures (Fig. 6.13), and is readily reversible (Quirk, 1994).

There are many examples in the literature showing that DLVO theory can account for the observed kinetic behavior of colloid systems (Napper and Hunter, 1974). However, this theory must be applied with caution since it treats ions exclusively as point charges and ignores their chemical properties.

The potential barrier preventing particles from coagulating is defined by the stability ratio (W), which is the fraction of the total number of collisions between particles that result in coagulation. The rate of coagulation in the absence of a potential barrier or rapid coagulation (R_f) is limited only by the rate of diffusion of the particles towards one another. When the particles have a potential barrier to overcome, the rate of coagulation (R_s) is slow and is related to R_f by:

$$R_s = \frac{R_f}{W} \qquad [6.39]$$

Rapid coagulation occurs when no significant repulsive forces act between particles and van der Waals or long-range coulombic attractions predominate. The quantification of the coagulation rate under these conditions was examined by von Smoluchowski (1916, 1917) and is discussed by Overbeek (1952).

Slow coagulation occurs over distances of the order of 1-100 nm when the approaching particles experience a barrier as their double layers overlap. Diffusion over this distance results from many individual Brownian events, some of which bring the particles closer together and some of which take them further apart. Since the rates of rapid and slow coagulation are directly proportional to the number of particles diffusing in the direction of a central particle (J), it follows from Equation [6.39] that the stability ratio is given by:

$$W = \frac{R_f}{R_s} = \frac{J_f}{J_s} = 2r\int_{2r}^{\infty} \exp\left(\frac{E_T}{K_B T}\right)\frac{dr}{d^2} \qquad [6.40]$$

where r is the particle radius and $d \cong 2r$. Verwey and Overbeek (1948) showed that W was determined almost entirely by the value of the total potential energy (E_T) at the maximum (Fig. 6.14). In Fig. 6.14, E_R and E_A are the potential energies due to repulsive and attractive forces. A more complete analysis of the kinetics of colloid flocculation is presented in Hunter (1987).

Gravity removes suspended particles by sedimentation while inducing differential sedimentation coagulation, thereby decreasing Brownian coagulation rates. Ultimately, sedimentation limits the time of a flocculation series test. The test should be long enough to detect relative changes in suspended particle numbers, but not so long that all dispersed particles settle from a stable suspension (Hesterberg and Page, 1990a).

The reverse of flocculation is called dispersion. Ideally, the amount of energy required to separate two particles coagulated into a potential energy minimum is approximately equal to the difference between the interaction energy at the minimum and that at the adjacent maximum (van Olphen, 1977). Under constant chemical conditions, separation of particles could presumably be induced by an input of kinetic energy (e.g., thermal or mechanical shear). Alternatively, changing the chemical conditions of the bulk solution surrounding coagulated particles could provide chemical and/or electrochemical energy to produce dispersion.

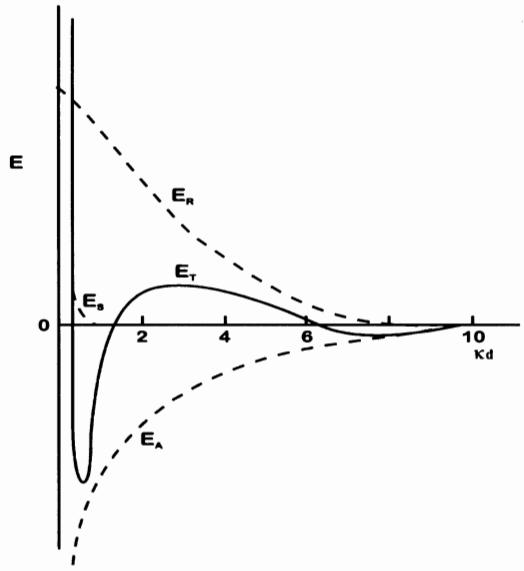

Fig. 6.14 Total potential energy of interaction of two colloidal particles: $E_T = E_S + E_R + E_A$, where E_S is the potential energy of repulsion due to the solvent layers, E_R is the potential energy due to the repulsive forces, and E_A is the potential energy due to the attractive forces, κD is particle separation [Reprinted by permission of Oxford University Press from Hunter, 1987. Foundations of colloid science Vol. 1]

6.3.1.1 Modes of Particle Association

Edge-Edge, Edge-Face, Face-Face

Clay crystals have a net negative surface charge as a consequence of isomorphic substitutions of electropositive elements for elements with a lower valence. This negative charge generates an ionic reorganization in the solution medium that has been described above as the double layer. Clay particles also have edge surfaces with atomic structure different from the faces. At the edge of the platelet, the tetrahedral sheet of Si and the octahedral layer of Al exhibit broken bonds which, in turn, generate another electric double layer.

Double layer theory assumes that the surfaces of the clay minerals are of semi-infinite spatial extent and show no edge effects, a simplification that is not always satisfactory. Clay mineral particles have finite dimensions. Below the p.z.c., edge surfaces carry a positive charge due to specific adsorption of protons. Using the Poisson-Boltzmann equation, Secor and Radke (1985) calculated the effect of edge-face corners on the electrical potential distribution around an idealized, symmetrical montmorillonite disk. Spillover of the negative electrical potential from the particle faces into the edge region can result in a negative potential everywhere around the particle.

The electrical potential at the edge surface strongly depends on the electrolyte concentration and the ratio of the face to edge charge density. The extent of spillover also is a weak function of the particle shape (Secor and Radke, 1985), which implies that attraction between positively charged edges and negatively charged faces of phyllosilicate mineral particles will depend on the extent of the edge protonation, electrolyte concentration, and shape of the particle. A phyllosilicate structure that is collapsed in the c-dimension, such as mica, should be able to acquire a larger edge surface charge density than a layer silicate like smectite where structural expansion increases the distance between edge surface aluminol groups (Hesterberg, 1988).

When there is a reduction in the thickness of the double layer, the particles can associate among themselves in three different ways: face-face, face-edge, or edge-edge. Face-face association is also called parallel aggregation and does not produce floccules while the other two associations do produce three-dimensional structures called card houses (Fig. 6.13).

In concentrated suspensions of clay, the edge-edge and edge-face associations form a continuum, with chains of particles in the card house structures mentioned above. The rigidity of the gel depends on the number and strength of the bonds in the continuum structure. Some attempts to characterize the gel structure using freeze drying techniques have been made (Norrish and Rausell-Colom, 1961). When the water is eliminated from the suspension, the volume of the system does not change and the final product is a dry clay structure with some strength that has been called aerogel (van Olphen, 1977).

Domains and Quasicrystals

Some colloidal systems may, under certain circumstances, show a reversible clustering among particles. The earliest reported example is the Fe hydroxide sol described by Cotton and Mouton (1907). The term tactoid was first used by Freundlich (1932) and was more precisely defined by Overbeek (1952) as the association of particles at a certain distance affected by electrolyte concentration and pH. Quirk and Aylmore (1971) proposed the term quasicrystal to describe the regions of parallel alignment of individual aluminosilicate lamellae in montmorillonite and the term domain to describe the regions of parallel alignment of crystals for illite which has been adopted in this chapter.

The distribution model of adsorbed ions in mixed mono- and divalent systems for smectite quasicrystals was described by Shainberg and Otoh (1968) and Bar-On et al. (1970). According to this theory, called the ion demixing model, when Na is added to Ca saturated montmorillonite, most of the adsorbed Na will concentrate on the external surfaces of the quasicrystals until 10% of the adsorbed Ca has been replaced by Na. Initially, the size and shape of the particles are not altered by the addition of adsorbed Na. As further Na is added to the system, Na penetrates into the quasicrystals and brings about disintegration of the clay packets (Bar-On et al., 1970).

Table 6.4 Critical coagulation concentrations of phyllosilicates under various conditions [Adapted from Hesterberg, 1988]

Mineral	CCC ($mol_c\ L^{-1}$)	Background electrolyte	pH	Solids concentration ($g\ kg^{-1}$)
Kaolinite-4	2-40	$NaNO_3$	4-10	0.025
Kaolinite-9	8, 30	$NaHCO_3$, Na_2CO_3	8.3, 9.5	0.6-0.9
Kaolinite (Georgia)	5, 245, 75	NaCl, $NaHCO_3$, Na_2CO_3	7, 8.3, 9.5	0.6-0.9
Kaolinite (KGa-1)	< 0.19-54.6	NaCl	5.8-9.1	0.67
Kaolinite-4	0.1-0.3	$Ca(NO_3)_2$	4-10	0.025
Montmorillonite-23	1-10	$NaNO_3$	3.8-10	0.25
Montmorillonite-23	20, 48, 68	NaCl, $NaHCO_3$, Na_2CO_3	7, 8.3, 9.5	0.6-0.9
Montmorillonite-27	14, 47,17	NaCl, $NaHCO_3$, Na_2CO_3	7, 8.3, 9.5	0.6-0.9
Montmorillonite (SAz-1)	14-28	NaCl	6.4-9.4	0.67
Montmorillonite (SAz-1)	1.09, 1.56	$CaCl_2$	6.1, 7.6	0.67
Montmorillonite (SAz-1)	0.93, 2.02, 0.88	$MgCl_2$	6.1, 8.4, 9.0	0.67
Vermiculite	38, 58, 30	NaCl, $NaHCO_3$, Na_2CO_3	7, 8.3, 9.5	0.6-0.9
Illite-36	9, 185, 95	NaCl, $NaHCO_3$, Na_2CO_3	7, 8.3, 9.5	0.6-0.9
Illite (Grundy)	7.24	NaCl	~ 6	1
Illite (Grundy)	0.2	$CaCl_2$	~ 6	1

Lebron and Suarez (1992a) used electrophoretic mobility experiments to show that the demixing model can be applied to micaceous clays. The electrophoretic mobility of micaceous domains increased when the sodium adsorption ratio (SAR) increased from 5 to approximately 10.

6.3.1.2 Critical Coagulation Concentration

The critical coagulation concentration (CCC) sometimes called the critical flocculation concentration (CFC) is the minimum concentration of indifferent electrolyte that induces rapid coagulation and is strongly dependent on counterion valence (Table 6.4). This observation is known as the Schulze-Hardy rule. An estimate of the CCC (mol L^{-1}) is given by (Hunter, 1987):

$$CCC = \frac{0.107\,\epsilon^3\,(K_B T)^5 Z^4}{N_A A_H^2 (ze)^6} \qquad [6.41]$$

where $Z = \tanh(ze\psi_0/4k_BT)$, N_A is Avogadro's number, A_H is the Hamaker constant, ϵ is the relative dielectric constant, k_B is the Boltzman constant, and e is the proton charge.

The variation of CCC with counterion valence depends approximately on the inverse sixth power of z. At 25°C in water, using the experimental observation that coagulation usually occurs between low potential surfaces, the result is

$$CCC \propto \frac{\psi_O^4}{z^2} \qquad [6.42]$$

where now the CCC depends on the inverse of the square of the valence. However, the CCC calculated with Equation [6.42] agrees well with experimental results if $\psi_0 \propto 1/z$. When calculating the CCC in soils, one must consider that soils consist of mixtures of permanent and variable charge minerals. The net surface charge, and consequently, the electrical potential around the mixture of particles are dependent upon variables such as pH, specifically adsorbed ions, ionic strength, and mineralogy. A more detailed evaluation of the effect of these variables on the stability of colloids is presented below.

6.3.2 Factors Affecting Colloidal Stability

6.3.2.1 Solution Composition

The magnitude of the repulsion barrier is determined by the nature of the material adsorbed on the particle surface. In the case of a charged colloid, repulsion depends on the magnitude of the surface charge and on the extent of the electrical double layer which, in turn, depends on the total electrolyte concentration. It is necessary here to distinguish between the concentration of the potential determining ions and that of other ions that have no direct interaction with the surface. If the surface potential of the particles is determined by the concentration of potential determining ions, the magnitude of this potential is not affected by the addition of an indifferent electrolyte. For this type of double layer, when salt concentration increases, the double layer thickness decreases, the surface charge of the particles increases, and the surface potential remains constant (Fig. 6.9a).

If the surface charge of the particle is determined by interior crystal imperfections, the surface charge does not change with increasing electrolyte concentration. The diffuse double layer compresses, but in this case, the surface potential decreases with increasing electrolyte concentration (Fig. 6.9b) (van Olphen, 1977).

6.3.2.2 Exchange Complex Composition

As explained above, clay particles are surrounded by cations as a consequence of the net negative electrical charge on the surface. Cations bonded to the surface can be exchanged for other cations in solution. Consequently, the cations on the exchange complex are dependent on the solution composition.

There is an equilibrium between the cations on the exchange complex and the cations in the solution. Not all the cations are adsorbed with the same affinity. Cations with larger hydrated radii are less strongly adsorbed than those with smaller radii. In solutions with equal initial concentrations of different cations, the amounts of Ca and Mg adsorbed are several times greater than the amount of Na adsorbed. In general, polyvalent cations are adsorbed more strongly than monovalent cations and are not easily displaced by other cations. The order of adsorption strength is Al > Ca > Mg > H > K > Na (Douchaufour, 1970).

The flocculation/dispersion behavior of soil colloids depends on salt concentration, exchange complex cation, cation valence, and dominant clay mineralogy. In general, divalent cations are more effective in flocculating colloids than monovalent cations. For example, Quirk and Schofield (1955) found that the flocculating power of $CaCl_2$ is 50 to 100 times higher than NaCl. For monovalent cations, there is also a difference, with KCl showing greater flocculation power than NaCl (Pashley, 1981).

6.3.2.3 pH

pH is an important determinant of the electrical potential of the clay surface. Changes in pH affect the edge charge on clays and the surface charge of variable charge minerals such as Fe and Al oxides. There is considerable variability depending on structural composition and degree of crystallinity, but Fe and Al oxides generally undergo a surface charge reversal around pH 7 to 9 (positively charged below that pH and negatively charged above). This is also the region in which kaolinite exhibits its edge charge reversal as evidenced by Cl^- adsorption studies (Schofield and Samson, 1954). Soil colloids consist of a mixture of minerals, each with a different p.z.c. At low pH, edge to face bonding, as well as bonding of positive Fe and Al oxides to negative clay surfaces is expected to occur (van Olphen, 1977; Kretzschmar et al., 1993, 1997). This type of bonding should hinder dispersion and should thus result in flocculation. With increasing pH, as the p.z.c. is approached, edge to face clay bonding decreases and Fe and Al hydrous oxide bonding to clays is also expected to decrease (Suarez et al., 1984). In variable charge systems, flocculation is at a maximum when the soil is at its p.z.c.

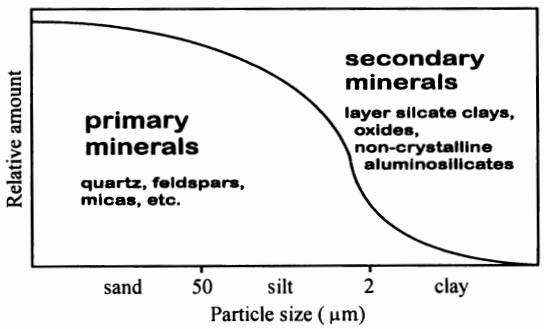

Fig. 6.15 Typical abundance of primary and secondary minerals in different size fractions of the soil [Reprinted from McBride, 1994. Environmental chemistry of soils. Copyright Oxford University Press, Inc. used by permission of Oxford University Press]

Critical coagulation concentration increased at high SAR values with increasing pH for three soil clays whose clay mineralogy was dominantly kaolinite, montmorillonite, or illite (Goldberg and Forster, 1990). Hesterberg and Page (1990b) found also an increase in CCC for a Na and a K illite with increasing pH. Similar results were found for illite and three micaceous soil clays when SAR > 15 (Lebron and Suarez, 1992a,b). The electrophoretic mobility of these materials increased when the SAR was higher than 20 and the pH was above the p.z.c. No pH effect was observed at SAR < 15 for either mobility or CCC.

6.3.2.4 Mineralogy

The colloidal fraction of a soil consists primarily of secondary minerals (Fig. 6.15). Layer silicate minerals differ in chemical composition and charge characteristics leading to different physico-chemical behavior (Tables 6.3 and 6.4). The stoichiometry of each mineral varies due to isomorphic substitutions in the crystal lattice during the formation or evolution of the mineral structure.

The siloxane (Si-O-Si) surfaces of 2:1 layer silicates without structural charge are hydrophobic. Therefore, the surface oxygens coordinated to Si shows little tendency to H bond with water molecules. Smectites, such as montmorillonite, with structural charge located mainly in the octahedral sheet form weak H bonds with water as a result of the delocalization of some structural charge into the surface oxygens (Farmer, 1978). Smectites, such as beidellite, with a high proportion of charge in the tetrahedral sheet form stronger H bonds. The siloxane surfaces of vermiculite are the most hydrophilic of the 2:1 layer silicate clays because they possess a large tetrahedral charge partially distributed onto surface oxygens (Farmer, 1978). Tetrahedral charge is much more localized on fewer surface oxygens than octahedral charge, explaining the stronger H bonding of adsorbed water on vermiculite (McBride, 1989). An extensive description of the structural characteristics of soil minerals can be found in Dixon and Weed (1989).

An example of how these mineral differences affect the flocculation/dispersion behavior of soil colloids is shown in Table 6.4. An overview of the data reveals that reported CCC values of kaolinite, montmorillonite, vermiculite, and illite are quite variable within and between these mineral groups.

Many of the differences in Table 6.4 are due to differences in methodology in the determination of CCC and/or differences in the stoichiometry of the silicate minerals. However, these factors do not account for all of the variability. Lebron and Suarez (1992a) found substantial differences in CCC within samples from the same soil type. Differences in content of organic matter and other minerals can drastically change the behavior of soil colloids. Consequently, general guidelines for reclamation of agricultural land or the use of amendments to maintain colloids in a flocculated state must be implemented with caution because soils usually require higher concentrations than the corresponding pure clay minerals to maintain a flocculated condition.

Table 6.5 Spatial extensions of electrical double layers and polymers of different molecular weight [Reprinted by permission of Oxford University Press from Hunter, 1987. Foundations of colloid science. Vol. 1]

1:1 Electrolyte concentration (mol L^{-1})	Double layer thickness, $1/\kappa$ (nm)	Polymer molecular weight	Spatial extension (nm)
10^{-5}	100	1,000,000	60
10^{-4}	30	100,000	20
10^{-3}	10	10,000	6
10^{-2}	3	1000	2
10^{-1}	1		

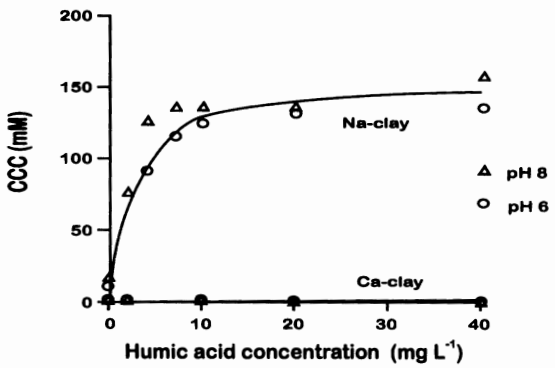

Fig. 6.16 Effect of humic acid concentration on the critical coagulation concentration (CCC) of a Na-clay and a Ca-clay [Used by permission of Oxford University Press, Inc. from Nelson and Oades, 1998. M.E. Sumner and R. Naidu (ed.) Sodic soils: Distribution, properties, management and environmental consequences. Copyright Oxford University Press, Inc.]

6.3.2.5 Organic Matter

Organic matter constitutes a small portion of the soil mass (0.5-10%) but is intimately associated with inorganic particles and plays an important role in the improvement of soil structure (Nelson and Oades, 1998). Aeration, water-holding capacity, and permeability increase when the SOM content increases in a soil. However, organic matter can promote dispersion of the soil particles. Organic coatings under certain conditions maintain a dispersed state for soil colloids in suspension through a combination of electrostatic and steric mechanisms (Stevenson, 1982). Table 6.5 shows the spatial extensions for non-ionic polymer molecules of different molecular weights. Like electrical double layers, macromolecules of at least a few thousand molecular weight also extend in space over distances comparable to, or greater than, the van der Waals attraction. When dissolved organic matter (DOM) adsorbs onto mineral surfaces, the humic substances behave as polyelectrolytes generating hydrophobic and hydrophilic surfaces (Hunter, 1987).

Goldberg and Forster (1990) and Kretzschmar et al. (1993) found that the removal of SOM enhanced soil flocculation (decreased the CCC). Similarly, addition of small amounts of organic material substantially increased dispersion of Na-saturated soil or clay in the order humic acid > soil polysaccharide ≥ anionic polysaccharide (Gu and Doner, 1993; Kretzschmar et al., 1997). Using smectite, kaolinite, and three soils whose clay fractions were dominated by one of these minerals, Frenkel et al. (1992) showed that the CCC values of Na-soils were much higher, and much more affected by organic matter than those of Ca soils. Tarchitzky et al. (1993) showed similar comparisons between Na and Ca montmorillonite suspensions with varying additions of humic and fulvic acids (Fig. 6.16). The effect of organic matter on stability of soil colloids is a function of its size. Large organic materials such as polysaccharides and hyphae act to bind colloid particles together. Small organic molecules such as fulvic acid and organic acids increase dispersion of soil colloids through their effect on particle charge. A more detailed review of organic matter chemistry and its effect on soils is provided in Stevenson (1982) and Nelson and Oades (1998).

6.3.3 Measurement of Colloidal Stability

6.3.3.1 Flocculation Series Test

Critical coagulation concentrations are commonly determined using the flocculation series test. The experiment can be performed by taking a series of test tubes containing the same concentration of the

colloid and adding varying amounts of the coagulating electrolyte. The tubes are then shaken quickly and allowed to stand for a given time. They are then briefly reshaken in order to remix the contents and again allowed to stand. If the electrolyte range has been properly chosen, the CCC is defined as the concentration above which the settling material leaves behind it a perfectly clear supernatant solution. Below the CCC, the supernatant retains some of the uncoagulated colloid. The concentration of colloidal particles, at which the flocculation test must be performed, should not exceed 10 g L^{-1}, thus avoiding interferences from different particle interactions such as gel formation.

6.3.3.2 Dispersion Indices

There are several methods (qualitative, semiquantitative, or quantitative) to determine the dispersion or flocculation status of soil colloids. Qualitative analyses are those based on direct observation of small particles when the soil is immersed in water. This observation can be made with the optical microscope or with the naked eye, as is the case for the test of Emerson (1967). Methods based on turbidity of a suspension of dispersed soil can be considered semiquantitative when comparative measurements are made. Normally, a standard curve is constructed using known amounts of dispersed clay. The soil under evaluation is assigned a dispersion value by comparison with the standard. The most commonly used quantitative method to determine soil flocculation state is the dispersion index which is the ratio of the amount of colloid in a water suspension after shaking to that when the soil has been treated with a dispersant. This procedure is recommended by the Soil Conservation Service (Sherard et al., 1977). Different variations regarding particle size, dispersing agent, and manipulation of samples are found in the methods proposed by Dong et al. (1983) and El-Swaify et al. (1970), among others.

6.3.3.3 Bingham Yield Stress

Rheology is the study of the flow and deformation of colloidal systems under the influence of mechanical forces (van Olphen, 1977). A Newtonian liquid when confined between two parallel plates moves at a constant shear rate ($\dot{\gamma}$) which is proportional to the applied shear stress (τ):

$$\tau = \eta\dot{\gamma} \qquad [6.43]$$

Non-Newtonian fluids obey different relations between shear stress and shear rate. Plastic flow is flow that occurs only above a certain finite stress (τ_0) called the yield stress. Ideal plastic flow exhibits a

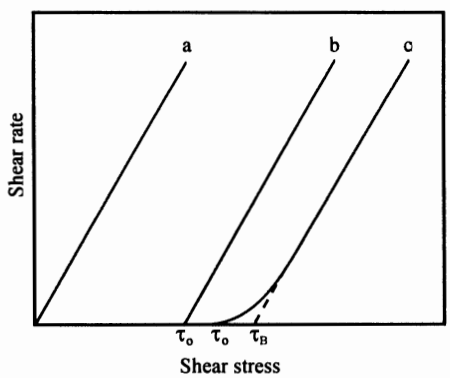

Fig. 6.17 Shear rate versus stress relationships. Curve a represents Newtonian flow, curve b represents ideal plastic flow, and curve c represents Bingham flow [Adapted from van Olphen, 1977]

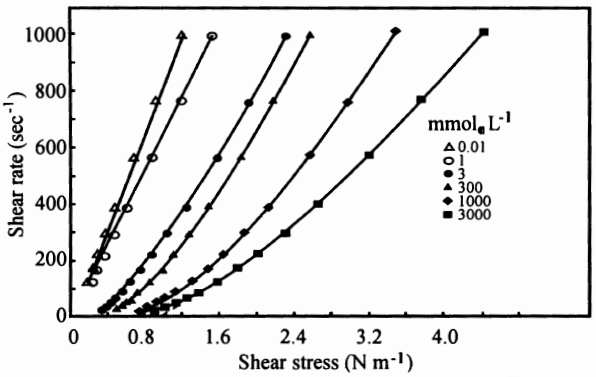

Fig. 6.18 Shear rate versus shear stress for Na-kaolinite. The open symbols represent dispersed systems and ideal plastic flow. The closed symbols represent coagulated systems and Bingham flow [Adapted from Yong et al., 1979]

linear relationship between shear rate and shear stress over all rates of shear. Many colloidal dispersions exhibit Bingham flow which is characterized by the equation:

$$\tau = \tau_B - \eta_\Delta \dot{\gamma} \qquad [6.44]$$

where τ_B is the Bingham yield stress found by extrapolating Equation [6.43] to zero shear rate and η_Δ is the differential or plastic viscosity. The differential viscosity is the derivative of shear stress with respect to shear rate at a given shear rate (van Olphen, 1977). Shear rate versus shear stress relationships for Newtonian, ideal plastic, and Bingham flow are presented in Fig. 6.17.

Bingham yield stress is a measure of the degree of coagulation of a colloidal suspension and the mode of particle interaction. Bingham yield stress is a function of both the number of particle-particle linkages in the coagulated structure and the energy required to break these linkages (Rand and Melton, 1977). A stable clay dispersion exhibits ideal plastic flow, while flocculated suspensions exhibit Bingham flow as can be seen in Fig. 6.18 for kaolinite. Differential viscosity can also be used to assess the extent of particle flocculation, but is a much less sensitive parameter than Bingham yield stress (Heath and Tadros, 1983).

Rheological studies have been carried out on kaolinite (Flegman et al., 1969; Rand and Melton, 1977; Yong et al., 1979; Diz and Rand, 1989), illite (Yong et al., 1979; Ohtsubo et al., 1991; Hesterberg and Page, 1993), montmorillonite (Rand et al., 1980; Heath and Tadros, 1983; Tombácz et al., 1989; Keren, 1988, 1989a), clay mixtures (Yong et al., 1979; Keren, 1989b, 1991), and soil clays (Zhao et al., 1991). A series of curves of Bingham yield stress as a function of pH obtained at successively increasing electrolyte concentration should coincide at one point. This point is characteristic of the pH value of the edge p.z.c. of the mineral (Rand and Melton, 1977). Edge p.z.c. values have been determined in this manner for various kaolinites and range in value from pH 5.6 to 8.8 (Diz and Rand, 1989). Kaolinite particles occur in edge-face associations below the edge p.z.c. and in edge-edge associations around the edge p.z.c. (Rand and Melton, 1977).

Montmorillonite exhibits no edge-face associations over the pH range 4 to 11; coagulation produced by electrolyte additions is initially the result of edge-edge interactions with face-face interactions occurring at high electrolyte concentrations (Rand et al., 1980). No edge p.z.c. could be determined on montmorillonite. This is likely because the edge area is small and attraction between edges and faces is small compared to repulsion between faces (Rand et al., 1980). In distilled water Ca

montmorillonite exhibited Newtonian flow. With increasing ESP, differential viscosity, deviation from Newtonian flow and Bingham yield stress of montmorillonite all increased (Keren, 1988). These increases are likely due to the increased number of particles in solution as tactoids break down. Differential viscosity and Bingham yield stress decreased with increasing electrostatic charge density of smectites (Keren, 1989a), which is attributed to the reduced swelling of higher charge density smectites. Kaolinite exhibited Newtonian flow at all ESPs. The introduction of even 5% montmorillonite into the kaolinite systems resulted in deviations from Newtonian flow and increased differential viscosity (Keren, 1989b). Bingham yield stress and deviations from Newtonian flow of kaolinite-montmorillonite mixtures also increased with ESP (Keren, 1991).

6.4 Colloid Transport

Colloid transport is important in predicting movement of organic chemicals, biological entities such as viruses and bacteria, inorganic species such as heavy metals, and clay movement which affects soil hydraulic properties. The colloids important to transport in soils include clay minerals, Fe, Mn, and Al oxyhydroxides, humic substances, bacteria, and viruses. Understanding colloid transport requires not only knowledge of the chemical and biological processes and reactions but also physical principles of filtration and deposition in porous media. In this section, both movement of the entity of interest as well as transport of a chemical after attachment to a colloid will be discussed.

In addition to the chemical factors affecting colloid stability, transport of colloids is related to soil physical factors such as pore size distribution and continuity. Coarse-textured soils have a larger distribution of pore sizes (with larger pores) than fine-textured soils; suggesting greater potential for colloid movement. This is not generalizable since some fine-textured materials experience cracking and formation of large macropores.

6.4.1 Principles of Colloid Transport

Various factors, both physical and chemical, affect the transport of colloids. Colloid transport can be represented by the physical processes of molecular diffusion (Brownian movement), liquid flow, and gravitational forces. Molecular diffusion, the random motion of particles caused by thermal effects is related to temperature and viscosity. The diffusion coefficient D is described by:

$$D = \frac{kt}{3\pi\eta d_p} \qquad [6.45]$$

where k is the Boltzmann constant, t is time, η is viscosity and d_p is particle diameter.
. Velocity differences within the fluid cause velocity differences in particle transport. These differences can result in interparticle contact. Gravitational forces within the moving fluid cause differential velocities among the particles, as related to their differences in density and size.

Filtration theory has been developed to describe the processes of aggregation and deposition, which can be readily adopted for colloid transport in soils. Aggregation is the term used to describe the attachment of particles which come in contact while moving. Deposition or coagulation is the process whereby moving particles are attached to stationary particles (O'Melia and Tiller, 1993). The rate of aggregation can be represented by:

$$\frac{dn}{dt} = -k_a n^2 \qquad [6.46]$$

where n is the concentration of the particles in the fluid and k_a is the rate constant which is a function of the physical and chemical properties of the system. Deposition can be described by the relation

$$\frac{dn}{dL} = -k_a n \qquad [6.47]$$

where L is distance in the flow path (O'Melia and Tiller, 1993). For a monodisperse suspension flowing into a clean filter bed, the rate of particle deposition can be described by:

$$\frac{dn}{dL} = -\frac{3}{2}\alpha_d \eta(p,c)\frac{(1-\theta)}{d_c} n \qquad [6.48]$$

where α_d is the dimensionless sticking coefficient (determined experimentally), $\eta(p,c)$ is the dimensionless collision frequency number for contact between the suspended particles and the filtering medium particles, θ is the porosity, and d_c is the diameter of the filtering media particles (O'Melia and Tiller, 1993). The collision frequency function is taken as the sum of the collisions from molecular diffusion, liquid flow, and gravitational processes.

Numerical treatment of colloid transport has ranged from relatively simple models to complex ones. Harvey and Garbadian (1991) developed the following simple model incorporating reversible and irreversible adsorption, as well as dispersion and advection at constant water content and velocity:

$$\theta\frac{\partial c}{\partial t} + \rho_b \frac{\partial s}{\partial t} = D\theta\frac{\partial^2 c}{\partial x^2} - v\theta\left(\frac{\partial c}{\partial x} + k_p c\right) \qquad [6.49]$$

where θ is the porosity, c is the concentration of the contaminant in solution, s is the concentration of reversibly adsorbed contaminant, D is the dispersion coefficient, v is the water velocity, t is time ρ_b is bulk density, x is the spatial coordinate and k_p is the irreversible adsorption constant.

Corapcioglu and Choi (1996) have recently developed a detailed model for description of colloid transport for unsaturated porous media. In this model, four phases are considered: air, water, solid, and colloids. The model considers both capture/release of the contaminant on the air-water interface as well as on the solid. Previous studies established that the air-water interface can be important in retention of colloids in soils (Wan and Wilson, 1994). Ibaraki and Sudicky (1995) describe a two-dimensional numerical model which includes colloid transport in fractured porous media.

6.4.2 Colloid Mediated Contaminant Transport

Numerous studies have established that organic and inorganic chemicals which are highly sorbed onto soil nonetheless are transported in the subsurface. Significant concentrations of colloids have been found in groundwaters. The major transport mechanism for colloids in groundwaters is considered to be convective diffusion (O'Melia, 1990), while convective transport is the major process for soils. Colloid mediated transport is, of course, dependent on the sorption processes. These processes are generally classified into two groups: equilibrium or instantaneous reactions, and slow or kinetically controlled reactions.

Many contaminants applied to soils were initially considered immobile, and thus, presenting little danger to groundwaters. Subsequently, it has been realized that migration of tightly held contaminants has occurred via colloid transport. Among these are metals, radionuclides, nonpolar organic contaminants, biomolecules such as viruses and bacteria, and macromolecular dissolved organic carbon. Transport of the contaminants should consider partitioning between the aqueous and solid phases and transport via dissolved and colloid movement. Treatment of colloid movement in soils must also consider that an important component of transport is by preferential flow, such as through macropores and cracks in the soil. Some of the general issues concerning contaminant migration by colloid facilitated transport are discussed in McCarthy and Zachara (1989). McDowell-Boyer et al. (1986) also provide a review of studies on contaminant transport.

Kaplan et al. (1993) examined the relation between colloid transport and flow rate for various soils packed into lysimeters. Increased flow rates increased colloid transport for all soils but the extent of increase varied greatly. Mobile colloids generally contained greater concentrations of organic C than did the bulk soil. This may explain the high negative charge of the colloids and their resultant stability in the aqueous phase.

Viruses range in size from 20 to 200 nm (Bitton, 1975). The surface charge of a virus is generated by the protonation/deprotonation of amino acid functional groups, The major charged functional entities are carboxyl, primary amine, and phenolic hydroxyl groups with the reactions given below (Taylor, 1981):

$$\begin{aligned} &-\mathrm{COOH} \rightleftharpoons -\mathrm{COO^-} + \mathrm{H^+} \\ &-\mathrm{NR_2H^+} \rightleftharpoons -\mathrm{NR_2} + \mathrm{H^+} \\ &\mathrm{Ph}-\mathrm{OH} \rightleftharpoons \mathrm{Ph}-\mathrm{O^-} + \mathrm{H^+} \end{aligned} \qquad [6.50]$$

These surfaces can be treated in a manner similar to variable charge mineral surfaces, discussed earlier. The particle charge can be determined using electrophoresis. Based on size (both of the bacteria and the size definition of a colloid) not all bacteria are strictly colloids, but they are nonetheless included in discussions of colloid transport since some of them are true colloids.

Among the studies on bacteria transport are those of Harvey and Garbadian (1991) who used Equation [6.49] in combination with the colloid filtration model to determine k_p as follows:

$$k_p = \frac{3}{2}\frac{(1-\theta)}{d}\alpha\eta_e \qquad [6.51]$$

where α is the collision efficiency factor, d is the diameter of the porous media grains, and η_e is the single collector efficiency. Yates and Yates (1991) provide further details on microbial transport modeling.

Radionuclide transport has been examined by Ryan et al. (1998), among others, who described Pu mobilization and subsurface transport under simulated rainfall conditions and observed the importance of macropore flow. Solution composition is an important factor affecting colloid-mediated transport in soils. Elevated pH and low ionic strength enhanced Ni transport related to colloid mobility despite the fact that elevated pH increased Ni sorption (Roy and Dzombak, 1997). Similarly, Grolimund et al. (1996) demonstrated that Pb^{2+} transport was dominantly associated with colloid mobility, the colloids being mobilized by a decrease in the ionic strength of the infiltrating water. Conditions of low ionic strength, high exchangeable Na and elevated pH all contribute to dispersion of clays and subsequent colloid transport (Kaplan et al., 1996). Prediction of clay colloid mobility is

thus related to the CCC value, allowing application of extensive data on the chemistry of dispersion and flocculation to colloid transport.

6.4.3 Effect of Colloid Transport on Hydraulic Conductivity

Reductions in hydraulic conductivity caused by colloid transport can be divided into two groups: formation of crusts and migration and deposition within the media. Crust formation results when the colloids are not able to enter the soil medium and form a compact layer above the soil. The description of this process and the resultant flow under saturated conditions can be treated using the filtration technology developed in the engineering literature. This process is called surface filtration (Herzig et al.,1970). Alternatively, the particles may enter the medium, flow with the water in a suspension, and be deposited within the medium. This process may result from either mechanical filtration of large colloids or physicochemical processes of attraction/repulsion of small colloids. Numerical description of the process under saturated flow, termed deep bed filtration (Herzig et al., 1970) is often made with a three-parameter model. The filter coefficient and the filtration efficiency parameters control the rate of deposition of the particles and the extent of removal of the particles from the suspension, respectively, while the flow restriction parameter is used to simulate the reduction in permeability (Ibaraki and Sudicky, 1995).

Research in soil science related to the effects of colloid transport on hydraulic conductivity has focused primarily on description of the chemical process affecting clay movement, rather than on mathematical expressions for prediction of flow rates. Conditions of low ionic strength, high exchangeable Na and elevated pH were related to both dispersion of clays (Goldberg and Forster, 1990; Miller et al., 1990; and Suarez et al., 1984) and subsequent migration and reduction in soil hydraulic conductivity (Suarez et al., 1984). In highly weathered acid soils where positively charged colloids are important, Seaman et al. (1995) determined that addition of $CaCl_2$ initially enhanced colloid mobility likely due to release of exchangeable Al and a decrease in pH.

6.4.4 Effect of Colloid Transport on Soil Formation

Soil profile development is often affected by colloid movement. Among these processes are the formation of impermeable clay layers in the subsurface and movement of Fe and Al, most probably as organic metal complexes. Moderately to strongly developed soils are generally characterized by depleted clay contents in the A horizon and larger amounts of clay generally in the upper portion of the B horizon. A substantial portion of the argillic B horizon is related to migration of clays from the upper portion of the profile and subsequent deposition (Birkeland, 1974). Flocculation in the lower part of the profile is enhanced by increased electrolyte concentration relative to the surface horizons. Clay colloid migration is evident by the presence of clay films over ped surfaces and inside voids and the presence of oriented clay particles. This process is also observed in Aridisols in which low organic matter and elevated exchangeable Na enhance colloid transport. Clay deposition is enhanced by increasing electrolyte concentration and removal of water by evapotranspiration. In general, formation of argillic horizons requires that the soil be at least partially dry during some part of the season.

Formation of Fe- and Al-rich layers by translocation (podzolization) is probably caused by transport of metal-fulvic acid complexes, rather than movement of the dissolved metals. The spodic B horizon marks the location at which these chelates either flocculate due to increases in electrolyte concentration or by decomposition of the organic matter (Birkeland, 1974).

6.5 References

Adamson, A.W. 1976. Physical chemistry of surfaces. 3rd ed. John Wiley and Sons, New York, NY.

Babcock, K.L. 1963. Theory of chemical properties of soil colloidal systems at equilibrium. Hilgardia 34:417–542.

Bar-On, P., I. Shainberg, and I. Michaeli. 1970. Electrophoretic mobility of montmorillonite particles saturated with Na/Ca ions. J. Coll. Interf. Sci. 33:471–472.

Beckett, R., and B.T. Hart. 1993. Use of field-flow fractionation techniques to characterize aquatic particles, colloids and macromolecules. p. 165–205. *In* J. Buffle and H.P. van Leeuwen (ed). Environmental Particles, Vol. 2. Lewis Publishers, Boca Raton, FL.

Beckett, R., D. Murphy, S. Tadjiki, D.J. Chittleborough, and J.C. Giddings. 1997. Determination of thickness, aspect ratio and size distribution for platey particles using sedimentation field-flow fractionation and electron microscopy. Coll. Surf. A 120:17–26.

Birkeland, P.W. 1974. Pedology, weathering, and geomorphological research. Oxford University Press, New York, NY.

Bitton, G. 1975. Adsorption of viruses onto surfaces in soil and water. Water Res. 9:473–484.

Bohn, H.L., B.L. McNeal, and G.A. O'Connor. 1985. Soil chemistry. John Wiley and Sons, New York, NY.

Borchardt, G.A. 1977. Montmorillonite and other smectite minerals. p. 293–330. *In* J.B. Dixon and S.B. Weed (ed.) Minerals in soil environments, Soil Science Society of America, Madison, WI.

Borkovec, M., Q. Wu, G. Degovics, P. Laggner, and H. Sticher. 1993. Surface area and size distribution of soil particles. Coll. Surf. A 73:65–76.

Bower, C.A., and J.O. Goertzen. 1959. Surface area of soils by an equilibrium ethylene glycol method. Soil Sci. 87:289–292.

Brown, G., A.C.D. Newman, J.H. Rayner, and A.H. Weir. 1978. The structure and chemistry of soil clay minerals. p. 29–178. *In* D.G. Greenland and M.H.B. Hayes (ed.) The chemistry of soil constituents, John Wiley and Sons, New York, NY.

Brunauer, S., P.H. Emmett, and E. Teller. 1938. Adsorption of gases in multimolecular layers. J. Am. Chem. Soc. 60:309–319.

Buffle, J., and G.G. Leppard. 1995a. Characterization of aquatic colloids and macromolecules. 1. Structure and behavior of colloidal materials. Environ. Sci. Technol. 29:2169–2175.

Buffle, J., and G.G. Leppard. 1995b. Characterization of aquatic colloids and macromolecules. 2. Key role of physical structures on analytical results. Environ. Sci. Technol. 29:2176–2184.

Bunville, L.G. 1984. Commercial instrumentation for particle size analysis. p. 1–42. *In* H.G. Barth (ed.) Modern methods of particle size analysis. John Wiley and Sons, New York, NY.

Carter, D.L., M.M. Mortland, and W.D. Kemper. 1986. Specific surface. p. 413–423. *In* A. Klute (ed.) Methods of soil analysis. Part 1. Physical and mineralogical methods. 2nd. Ed. Soil Science Society of America, Madison, WI.

Chorom, M., and P. Rengasamy. 1995. Dispersion and zeta potential of pure clays as related to net particle charge under varying pH, electrolyte concentration and cation type. Europ. J. Soil Sci. 46:657–665.

Coll, H., and L.E. Oppenheimer. 1987. Improved techniques in disc centrifugation. p. 202–214. *In* T. Provder (ed.) Particle size distribution. Assessment and characterization. American Chemical Society, Washington, DC.

Corapcioglu, M.Y., and H. Choi. 1996. Modeling colloid transport in unsaturated porous media and validation with laboratory column data. Water Resour. Res. 32:3437–3449.

Cotton, A., and H. Mouton. 1907. Magneto-optical properties of colloids and heterogeneous liquids. Ann. Chim. Phys. 11:145–203, 289–339.

Davis, J.A., and J.D. Hem. 1989. The surface chemistry of aluminum oxides and hydroxides. p. 185–219. *In* G. Sposito (ed.) The environmental chemistry of aluminum. CRC Press, Boca Raton, FL.

Davis, J.A., and D.B. Kent. 1990. Surface complexation modeling in aqueous geochemistry. Rev. Mineral. 23:177–260.

Dixon, J.B. 1977. Kaolinite and serpentine group minerals. p. 357–403. *In* J.B. Dixon and S.B. Weed (ed.) Minerals in soil environments. Soil Science Society of America, Madison, WI.

Dixon, J.B., and S.B. Weed. 1989. Minerals in soil environments. Soil Science Society of America, Madison, WI.

Diz, H.M.M., and B. Rand. 1989. The variable nature of the isoelectric point of the edge surface of kaolinite. British Ceram. Trans. J. 88:162–166.

Dong, A., G. Chesters, and G.V. Simsiman. 1983. Soil dispersibility. Soil Sci. 136:208–212.

Douchafour, P. 1970. Precis de pedologie. Masson et Cie, Paris, France.

Douglas, L.A. 1977. Vermiculites. p. 259–292. *In* J.B. Dixon and S.B. Weed (ed.) Minerals in soil environments. Soil Science Society of America, Madison, WI.

Ducker, W.A., and R.M. Pashley. 1992. Forces between mica surfaces in the presence of rod-shaped divalent counterions. Langmuir 8:109–112.

Dyal, R.S., and S.B. Hendricks. 1950. Total surface of clays in polar liquids as a characteristic index. Soil Sci. 69:421–432.

Dzombak, D.A., and F.M.M. Morel. 1990. Surface complexation modeling: Hydrous ferric oxide. John Wiley and Sons, New York, NY.

Edwards, D.G., A.M. Posner, and J.P. Quirk. 1965a. Repulsion of chloride ions by negatively charged clay surfaces. Part 1. Monovalent cation Fithian illites. Trans. Farad. Soc. 61:2808–2815.

Edwards, D.G., A.M. Posner, and J.P. Quirk. 1965b. Repulsion of chloride ions by negatively charged clay surfaces. Part 2. Monovalent montmorillonites. Trans. Farad. Soc. 61:2816–2819.

El-Swaify, S.A., S. Ahmed, and L.D. Swindale. 1970. Effects of adsorbed cations on physical properties of tropical red and tropical black earths. II. Liquid limit, degree of dispersion, and moisture retention. J. Soil Sci. 21:188–198.

Emerson, W.W. 1967. A classification of soil aggregates based on their coherence in water. Aust. J. Soil Res. 15:255–262.

Fanning, D.S., and V.Z. Keramidas. 1977. Micas. p. 195–258. *In* J.B. Dixon and S.B. Weed (ed.) Minerals in soil environments. Soil Science Society of America, Madison, WI.

Farmer, V.C. 1978. Water on particle surfaces. p. 405–448. *In* D.J. Greenland and M.H.B. Hayes (ed.) The chemistry of soil constituents. John Wiley and Sons, New York, NY.

Filella, M., and J. Buffle. 1993. Factors controlling the stability of submicron colloids in natural waters. Coll. Surf. A 73:255–273.

Filella, M., J. Zhang, M.E. Newman, and J. Buffle. 1997. Analytical applications of photoncorrelation spectroscopy for size distribution measurements of natural colloidal suspensions: capabilities and limitations. Coll. Surf. A. 120:27–46.

Flegman, A.W., J.W. Goodwin, and R.H. Ottewill. 1969. Rheological studies on kaolinite suspensions. Proc. British Ceram. Soc. 13:31–45.

Frenkel, H., G.J. Levy, and M.V. Fey. 1992. Clay dispersion and hydraulic conductivity of clay-sand mixtures as affected by the addition of various anions. Clays Clay Miner. 40:515–521.

Freundlich, H. 1932. Kapillarchemie II. Eine Darstellung der Chemie der Kolloide und verwandter Gebiete. 4. Akademische Verlagsgesellschaft. Leipzig, Germany.

Giddings, J.C., K.D. Cadwell, and H.K. Jones. 1987. Measuring particle size distribution of simple and complex colloids using sedimentation field-flow fractionation. p. 215–230. *In* T. Provder (ed.) Particle size distribution. Assessment and characterization. American Chemical Society, Washington, DC.

Goldberg, S., and H.S. Forster. 1990. Flocculation of reference clays and arid-zone soil clays. Soil Sci. Soc. Am. J. 54:714–718.

Goldberg, S., H.S. Forster, and C.L. Godfrey. 1996. Molybdenum adsorption on oxides, clay minerals, and soils. Soil Sci. Soc. Am. J. 60:425–432.

Greathouse, J.A., S.E. Feller, and D.A. McQuarrie. 1994. The modified Gouy-Chapman theory: Comparisons between electrical double layer models of clay swelling. Langmuir 10:2125–2130.

Gregg, S.J., and K.S. W. Sing. 1982. Adsorption, surface area and porosity. Academic Press, New York, NY.

Grolimund, D., M. Borkovec, K. Bartmettler, and H. Sticher. 1996. Colloid-facilitated transport of strongly sorbing contaminants in natural porous media: A laboratory column study. Environ. Sci. Technol. 30:3118–3123.

Groves, M.J. 1984. The application of particle characterization methods to submicron dispersion and emulsions. p. 43–91. *In* H.G. Barth (ed.) Modern methods of particle size analysis. John Wiley and Sons, New York, NY.

Gu, B., and H.E. Doner. 1993. Dispersion and aggregation of soils as influenced by organic and inorganic polymers. Soil Sci. Soc. Am. J. 57:709–716.

Harvey, R.W., and S.P. Garbadian. 1991. Use of colloid filtration theory in modeling movement of bacteria through a contaminated sandy aquifer. Environ. Sci. Technol. 25:178–185.

Hayes, M.H.B., and R.S. Swift. 1978. The chemistry of soil organic colloids. p. 179–320. *In* D.G. Greenland and M.H.B. Hayes (eds.) The chemistry of soil constituents. John Wiley and Sons, New York, NY.

Heath, D., and Th.F. Tadros. 1983. Influence of pH, electrolyte and poly(vinyl alcohol) addition on the rheological characteristics of aqueous dispersions of sodium montmorillonite. J. Coll. Interf. Sci. 93:307–319.

Herzig, J.P., D.M. Leclerc, and P. Le Groff. 1970. Flow of suspensions through porous media: Applications to deep filtration. Ind. Eng. Chem. 62:8–35.

Hesterberg, D.L. 1988. Critical coagulation concentrations and rheological properties of illite. Ph.D. Thesis. University of California, Riverside CA.

Hesterberg, D., and A.L. Page. 1990a. Flocculation series test yielding time-invariant critical coagulation concentrations of sodium illite. Soil Sci. Soc. Am. J. 54:729–735.

Hesterberg, D., and A.L. Page. 1990b. Critical coagulation concentration of sodium and potassium illite as affected by pH. Soil Sci. Soc. Am. J. 54:735–739.

Hesterberg, D., and A.L. Page. 1993. Rheology of sodium and potassium illite suspensions in relation to colloidal stability. Soil Sci. Soc. Am. J. 57:697–704.

Hiemenz, P.C. 1977. Principles of colloid and surface chemistry. Marcel Dekker, Inc., New York, NY.

Holsworth, R.M., T. Provder, and J.J. Stansbrey. 1987. External-gradient-formation method for disc centrifuge photosedimentometric particle size distribution analysis. p. 191–201. *In* T. Provder (ed.) Particle size distribution. Assessment and characterization. American Chemical Society, Washington, DC.

Hsu, P.H. 1977. Aluminum hydroxides and oxyhydroxides. p. 99–143. *In* J.B. Dixon and S.B. Weed (ed.) Minerals in soil environments. Soil Science Society of America, Madison, WI.

Huang, C.P. 1981. The surface acidity of hydrous solids. p. 183–217. *In* M.A. Anderson and A.J. Rubin (ed.) Adsorption of inorganics at solid-liquid interfaces. Ann Arbor Science, Ann Arbor, MI.

Hunter, R.J. 1981. Zeta potential in colloid science. Academic Press, London, UK.

Hunter, R.J. 1987. Foundations of colloid science. Vol. 1. Oxford University Press, New York, NY.

Hunter, R.J. 1989. Foundations of colloid science. Vol. 2. Oxford University Press, New York, NY.

Hunter, R.J. 1993. Introduction to modern colloid science. Oxford Science Publications, Oxford, UK.

Hutton, J.T. 1977. Titanium and zirconium minerals. p. 673–688. *In* J.B. Dixon and S.B. Weed (ed.) Minerals in soil environments. Soil Science Society of America, Madison, WI.

Ibaraki, M., and E.A. Sudicky. 1995. Colloid-facilitated contaminant transport in discretely fractured porous media. I. Numerical formulation and sensitivity analysis. Water Resour. Res. 31:2945–2960.

Israelachvili, J.N. 1992. Intermolecular and surface forces. 2nd Ed. Academic Press, London, UK.

Jackson, M.L. 1979. Soil chemical analysis: Advanced course. 2nd Ed. Published by the author, Madison, WI.

James, R.O., and G.A. Parks. 1982. Characterization of aqueous colloids by their electrical double-layer and intrinsic surface chemical properties. Surf. Coll. Sci. 12:119–126.

Kaplan, D.I., P.M. Bertsch, D.C. Adriano, and W.P. Miller. 1993. Soil-borne colloids as influenced by water flow and organic carbon. Environ. Sci. Technol. 27:1193–1200.

Kaplan, D.I., M.E. Sumner, P.M. Bertsch, and D.C. Adriano. 1996. Chemical conditions conducive to the release of mobile colloids from Ultisol profiles. Soil Sci. Soc. Am. J. 60:269–274.

Kavanaugh, M.C., and J.O. Leckie. 1980. Particulates in water. American Chemical Society, Washington, DC.

Kavanaugh, M.C., C.H.Tate, A.R. Trussell, R. R. Trussell, and G. Treweek. 1980. Use of particle size distribution measurements for selection and control of solid/liquid separation processes. p. 305–328. *In* M.C. Kavanaugh and J.O. Leckie (ed.) Particulates in water. American Chemical Society, Washington, DC.

Kékicheff, P., S. Marcelja, T.J. Senden, and V.E. Shubin. 1993. Charge reversal seen in electrical double layer interaction of surfaces immersed in 2:1 calcium electrolyte. J. Chem. Phys. 99:6098–6113.

Keren, R. 1988. Rheology of aqueous suspension of sodium/calcium montmorillonite. Soil Sci. Soc. Am. J. 52:924–928.

Keren, R. 1989a. Effect of clay charge density and adsorbed ions on the rheology of montmorillonite suspension. Soil Sci. Soc. Am. J. 53:25–29.

Keren, R. 1989b. Rheology of mixed kaolinite-montmorillonite suspensions. Soil Sci. Soc. Am. J. 53:725–730.

Keren, R. 1991. Adsorbed sodium fraction's effect on rheology of montmorillonite-kaolinite suspensions. Soil Sci. Soc. Am. J. 55:376–379.

Koehler, M.E., R.A. Zandler, T. Gill, T. Provder, and T.F. Niemann. 1987. An improved disc centrifuge photosedimentometer and data system for particle size distribution analysis. p. 180–190. *In* T. Provder (ed.) Particle size distribution. Assessment and characterization. American Chemical Society, Washington, DC.

Kretzschmar, R., W.P. Robarge, and S.B. Weed. 1993. Flocculation of kaolinitic soil clays: Effects of humic substances and iron oxides. Soil Sci. Soc. Am. J. 57:1277–1283.

Kretzschmar, R, D. Hesterberg, and H. Sticher. 1997. Effects of adsorbed humic acid on surface charge and flocculation of kaolinite. Soil Sci. Soc. Am. J. 61:101–108.

Langmuir, I. 1918. The adsorption of gases on plane surfaces of glass, mica, and platinum. J. Am. Chem. Soc. 40:1361–1402.

Lebron I., and D.L. Suarez. 1992a. Electrophoretic mobility of illite and micaceous soil clays. Soil Sci. Soc. Am. J. 56:1106–1115.

Lebron I., and D.L. Suarez. 1992b. Variations in soil stability within and among soil types. Soil Sci. Soc. Am. J. 56:1412–1421.

Lebron, I., D.L. Suarez, C. Amrhein, and J.E. Strong. 1993. Size of mica domains and distribution of the adsorbed Na-Ca ions. Clays Clay Miner. 41:380–388.

Ledin, A., S. Karlsson, A. Duker, and B. Allard. 1993. Applicability of photon correlation spectroscopy for measurement of concentration and size distribution of colloids in natural waters. Anal. Chem. Acta 281:421–428.

Lowell, S. 1979. Introduction to powder surface area. John Wiley and Sons, New York, NY.

Maes, A., and A. Cremers. 1977. Charge density effects in ion exchange. Part 1. Heterovalent exchange equilibria. J. Chem. Soc. Faraday Trans. I 73:1807–1814.

McBride, M.B. 1989. Surface chemistry of soil minerals. p. 35–88. *In* J.B. Dixon and S.B. Weed (ed.) Minerals in soil environments. 2nd Ed., Soil Science Society of America, Madison, WI.

McBride, M.B. 1994. Environmental chemistry of soils. Oxford University Press, New York, NY.

McCarthy, J.E., and J.M. Zachara. 1989. Subsurface transport of contaminants. Environ. Sci. Technol. 23:496–502.

McDowell-Boyer, L.M., J.R. Hunt, and N. Sitar. 1986. Particle transport through porous media. Water Resour. Res. 22:1901–1921.

McKenzie, R.M. 1989. Manganese oxides and hydroxides. p. 439–465. *In* J.B. Dixon and S.B. Weed (ed.) Minerals in soil environments. 2nd Ed. Soil Science Society of America, Madison, WI.

Miller, W.P., H. Frenkel, and K.D. Newman. 1990. Flocculation concentration and sodium/calcium exchange of kaolinitic soil clays. Soil Sci. Soc. Am. J. 54:346–351.

Napper, D.H., and R.J. Hunter. 1974. Hydrosols. p.161–213. *In* M. Kerker (ed.) M.T.P. Int. Review of Science Phys. Chem. Series. Butterworths, London, UK.

Nelson, P.N., and J.M. Oades. 1998. Organic matter, sodicity and soil structure. p. 67–84. *In* Sodic Soils. M.E. Sumner and R. Naidu (ed.) Oxford University Press, New York, NY.

Nishimura, S., H. Tateyama, K. Tsunematsu, and K. Jinnai. 1992. Zeta potential measurement of muscovite mica basal plane-aqueous solution interface by means of plane interface technique. J. Coll. Interf. Sci. 152:359–367.

Ohtsubo, M., A. Yoshimura, S.-I. Wada, and R.N. Yong. 1991. Particle interaction and rheology of illite-iron oxide complexes. Clays Clay Miner. 39:347–354.

O'Melia, C.R. 1990. Kinetics of colloid chemical processes in aquatic systems. p. 447–422. *In* W. Stumm (ed.) Aquatic chemical kinetics. Reaction rates of processes in natural waters. Wiley Interscience, New York, NY.

O'Melia, C.R, and C.L. Tiller. 1993. Physicochemical aggregation and deposition in aquatic environments. p. 353–385. *In* J. Buffle and H. van Leeuwen (ed.) Environmental particles. Vol. 2. Lewis Publishers, Boca Raton, FL.

Norrish, K., and J.A. Rausell-Colom. 1961. Low-angle X-ray diffraction studies of the swelling of montmorillonite and vermiculite. Clays Clay Min. 10:123–149.

Overbeek, J.Th.G. 1952. Stability of hydrophobic colloids and emulsions. Coll. Sci. 1:302–341.

Parker, J.C., L.W. Zelazny, S. Sampath, and W.G. Harris. 1979. A critical evaluation of the extension of zero point of charge (ZPC) theory to soil systems. Soil Sci. Soc. Am. J. 43:668–674.

Pashley, R.M. 1981. DLVO and hydration forces between mica surfaces in Li^+, Na^+, K^+, and Cs^+ electrolyte solutions: A correlation of double-layer and hydration forces with surface cation. J. Coll. Interf. Sci. 83:531–546.

Pecora, R. 1983. Quasi-elastic light scattering of macromolecules and particles in solution and suspension. p. 3–30. *In* B.E. Dahneke (ed.) Measurement of suspended particles by quasi-elastic light scattering. John Wiley and Sons, New York, NY.

Pham, P.T., and G.W. Brindley. 1970. Methylene blue adsorption by clay minerals: Determination of surface areas and cation exchange capacities. Clays Clay Miner. 18:203–212.

Quirk, J.P. 1994. Interparticle forces: A basis for the interpretation of soil physical behavior. Adv. Agron. 53:121–183.

Quirk, J.P., and L.A.G. Aylmore. 1971. Domain and quasi-crystalline regions in clay systems. Soil Sci. Soc. Am. Proc. 35:652–654.

Quirk, J.P., and R.K. Schofield. 1955. The effect of electrolyte concentration on soil permeability. J. Soil Sci. 6:163–178.

Rand, B., and I.E. Melton. 1977. Particle interactions in aqueous kaolinite suspensions. I. Effect of pH and electrolyte upon the mode of particle interaction in homoionic sodium kaolinite suspensions. J. Coll. Interf. Sci. 60:308–320.

Rand, B., E. Pekenc, J.W. Goodwin, and R.W. Smith. 1980. Investigation into the existence of edge-face coagulated structures in Na-montmorillonite suspensions. J. Chem. Soc. Farad. I. 76:225–235.

Ross, G. 1978. Relationships of specific surface area and clay content to shrink-swell potential of soils having different clay mineralogical compositions. Can. J. Soil Sci. 58:159–166.

Roy, S.B., and D.A. Dzombak. 1997. Chemical factors influencing colloid-facilitated transport of contaminants in porous media. Environ. Sci. Technol. 37:656–664.

Ryan, J.N., T.H. Illangasekare, M.I. Litaor, and R. Shannon. 1998. Particle and plutonium mobilization in macroporous soils during rainfall simulations. Environ. Sci. Technol. 32:476–482.

Scales, P.J., F. Grieser, and T.W. Healy. 1990. Electrokinetics of the muscovite mica-aqueous solution interface. Langmuir 6:582–589.

Schofield, R. K. 1949. Calculation of surface areas of clays from measurements of negative adsorption. Trans. British Ceramic Soc. 48:207–213.

Schofield, R.K., and H.R. Samson. 1954. Flocculation of kaolinite due to the attraction of oppositely charged crystal faces. Disc. Farad. Soc. 18:135–145.

Schramm L.L., and J.C.T. Kwak. 1982. Influence of exchangeable cation composition on the size and shape of montmorillonite particles in dilute suspensions. Clays Clay Miner. 30:40–48.

Schulthess, C.P., and D.L. Sparks. 1986. Backtitration technique for proton isotherm modeling of oxide surfaces. Soil Sci. Soc. Am. J. 50:1406–1411.

Schulze, D.G. 1989. An introduction to soil mineralogy. p. 1–34. *In* J.B. Dixon and S.B. Weed (ed.). Minerals in soil environments. 2nd Ed. Soil Science Society of America, Madison, WI.

Schurtenberger, P., and M.E. Newman. 1993. Characterization of biological and environmental particles using static and dynamic light scattering. p. 37–115. *In* J. Buffle and H.P. van Leeuwen (ed.). Environmental particles, Vol. 2. Lewis Publishers, Boca Raton, FL.

Schwertmann, U., and R.M. Taylor. 1977. Iron oxides. p. 145–180. *In* J.B. Dixon and S.B. Weed (ed.) Minerals in soil environments. Soil Science Society of America, Madison, WI.

Seaman, J.C., P.M. Bertsch, and W.P. Miller. 1995. Chemical controls on colloid generation and transport in a sandy aquifer. Environ. Sci. Technol. 29:1808–1815.

Secor, R.B., and C.J. Radke. 1985. Spillover of the diffuse double layer on montmorillonite particles. J. Coll. Interf. Sci. 103:237–244.

Shainberg, I., and H. Otoh. 1968. Size and shape of montmorillonite particles saturated with Na/Ca ions (inferred from viscosity and optical measurements). Israel J. Chem. 6:251–259.

Shapiro, A.P., and R.F. Probstein. 1993. Removal of contaminants from saturated clay by electroosmosis. Environ. Sci. technol. 27:283–291.

Sherard, J.L., L.P. Dunningan, and R.S. Decker. 1977. Identification and nature of dispersive soils. J. Geotech. Eng., Am. Soc. Chem. Eng. 4:287–301.

Sposito, G. 1984. The surface chemistry of soils. Oxford University Press, New York, NY.

Stevenson, F.J. 1982. Humus chemistry. Genesis, composition, reactions. John Wiley and Sons, New York, NY.

Stumm, W., and J.J. Morgan. 1996. Aquatic chemistry. Chemical equilibria and rates in natural waters. John Wiley and Sons, New York, NY.

Suarez, D.L., J.D. Rhoades, R. Lavado, and C.M. Grieve. 1984. Effect of pH on saturated hydraulic conductivity and soil dispersion. Soil Sci. Soc. Am. J. 48:50–55.

Supak, J.R., A.R. Swoboda, and J.B. Dixon. 1978. Adsorption of aldicarb by clays and soil organo-clay complexes. Soil Sci. Soc. Am. J. 42:244–248.

Tarchitzky, J., Y. Chen, and A. Banin. 1993. Humic substances and pH effects on sodium and calcium-montmorillonite flocculation and dispersion. Soil Sci. Soc. Am J. 57:367–372.

Taylor, D. 1981. Interpretation of the adsorption of viruses by clays from their electrokinetic properties. p. 595–612. *In* J.U. Cooper (ed.) Chemistry in water reuse. Ann Arbor Science, Ann Arbor, MI.

Tombácz, E., J. Balázs, J. Lakatos, and F. Szántó. 1989. Influence of the exchangeable cations on stability and rheological properties of montmorillonite suspensions. Colloid Polym. Sci. 267:1016–1025.

van Olphen, H. 1977. An introduction to clay colloid chemistry. 2nd Ed. John Wiley and Sons, New York, NY.

Verwey, E.J.W., and J.Th.G. Overbeek. 1948. Theory of stability of lyophobic colloids. Elsevier, Amsterdam, Netherlands.

von Smoluchowski, M. 1916. Three discourses on diffusion, Brownian movements, and the coagulation of colloid particles. Physik. Z.17:557–571; 585–599.

von Smoluchowski, M. 1917. Mathmetical theory of the kinetics of the coagulation of colloidal solutions. Z. Physik. Chem. 92:129–168.

Wan, J., and J.L. Wilson. 1994. Colloid transport in unsaturated porous media. Water Resour. Res. 30:857–864.

Wilding, L.P., N.E. Smeck, and L.R. Drees. 1977. Silica in soils: Quartz, cristobalite, tridymite, and opal. p. 471–552. *In* J.B. Dixon and S.B. Weed (ed.) Minerals in soil environments. Soil Science Society of America, Madison, WI.

Yates, M.V. and S.R. Yates. 1991. Modeling microbial transport in the subsurface: A mathematical discussion. p. 48–76. *In* C.J. Hurst (ed.). Modeling the environmental fate of microorganisms. American Society for Microbiology, Washington, DC.

Yong, R.N., A.J. Sadh, H.P. Ludwig, and M.A. Jorgensen. 1979. Interparticle action and rheology of dispersive clays. J. Geotech. Eng. Div. 105:1193-1209.

Zhao, H., P.F. Low, and J.M. Bradford. 1991. Effects of pH and electrolyte concentration on particle interaction in three homoionic sodium soil clay suspensions. Soil Sci. 151:196–207.